Geoneutrino Observation

Tadao Mitsui
Research Center for Neutrino Science,
Tohoku University

Sixteenth Marcel Grossmann Meeting
July 6, 2021
Rome (online)

Geoneutrino

- Geoneutrino as a new probe to observe Earth's interior
- Predicted more than 50 years ago
- Geoneutrino observation has been done with KamLAND and Borexino.

Geoneutrino as a new probe to observe Earth's interior

Seismic wave and geoneutrino

- Seismic wave is the strongest tool to see Earth's interior, but it has been a lonely tool for long time.

- Geoneutrino is the first independent, compensating, synergetic companion, which will provide new information, such as heat source amount, and chemical composition.

Geo-neutrino source: ^{238}U series

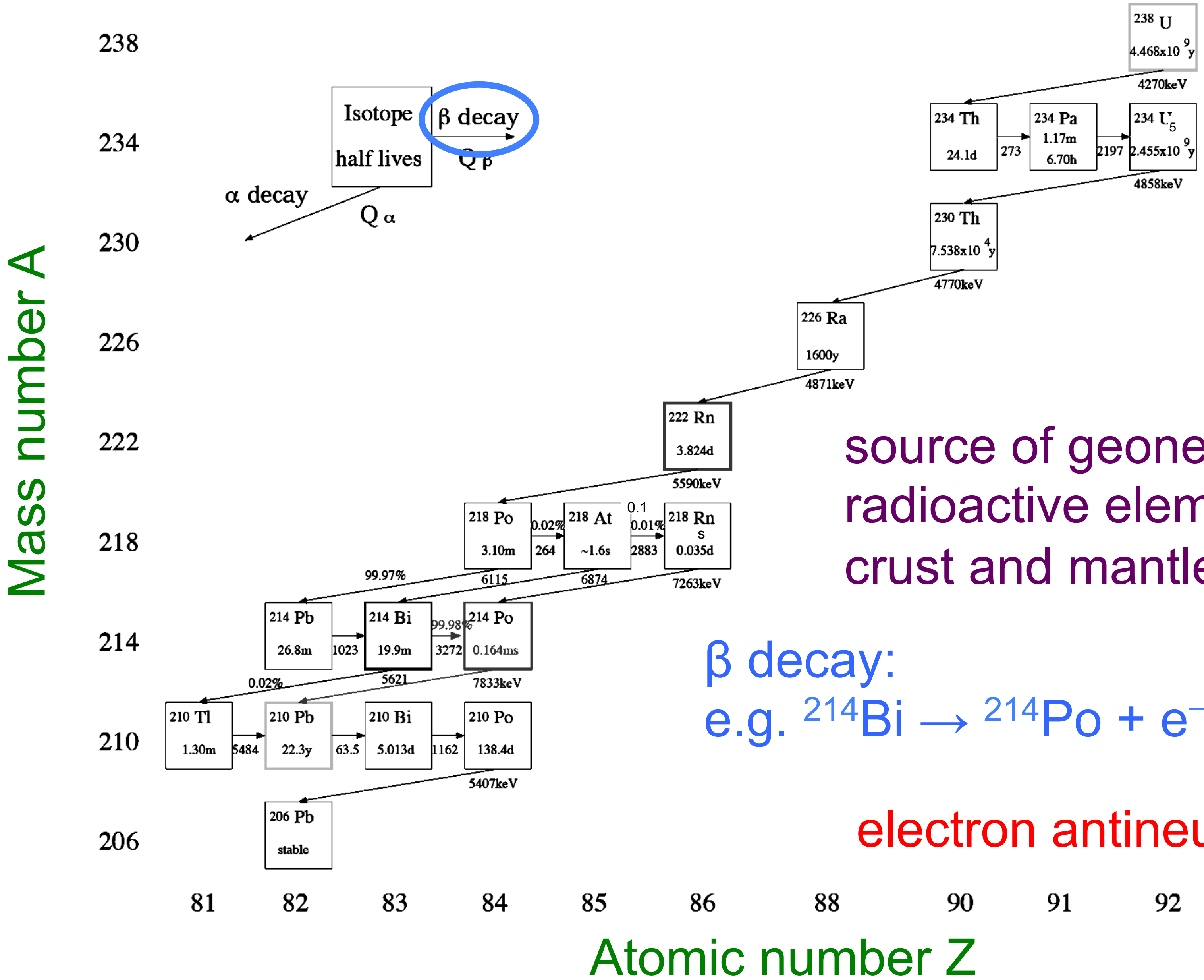

source of geoneutrino: radioactive element in the crust and mantle

β decay:
e.g. $^{214}\mathrm{Bi} \rightarrow {}^{214}\mathrm{Po} + e^{-} + \overline{\nu}_e$

electron antineutrino

Geo-neutrino source: ^{232}Th series

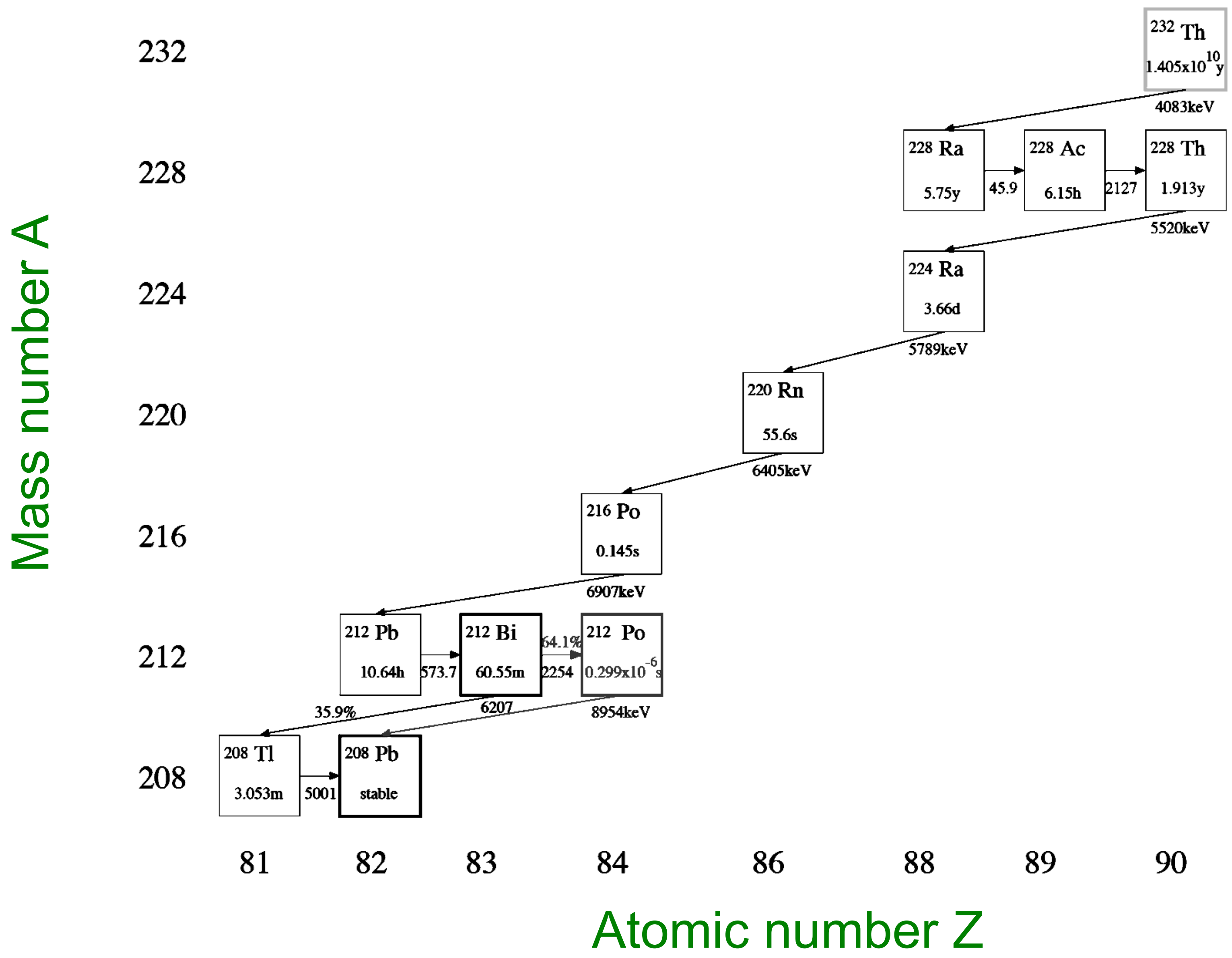

Geoneutrino from ^{238}U, ^{232}Th, ^{40}K

Half life

$$^{238}\mathrm{U} \xrightarrow[100\%]{} {}^{206}\mathrm{Pb} + 8\,{}^{4}\mathrm{He} + 6e^{-} + \underline{6\bar{\nu}_e} + 51.7\ [\mathrm{MeV}]$$

4.47 Gy

$$^{232}\mathrm{Th} \xrightarrow[100\%]{} {}^{208}\mathrm{Pb} + 6\,{}^{4}\mathrm{He} + 4e^{-} + \underline{4\bar{\nu}_e} + 42.7\ [\mathrm{MeV}]$$

14.05 Gy

$$^{40}\mathrm{K} \xrightarrow[89.28\%]{} {}^{40}\mathrm{Ca} + e^{-} + \underline{\bar{\nu}_e} + 1.311\ [\mathrm{MeV}]$$

1.28 Gy

$$^{40}\mathrm{K} + e^{-} \xrightarrow[10.72\%]{} {}^{40}\mathrm{Ar} + \nu_e + 1.505\ [\mathrm{MeV}]$$

- Electron antineutrino ($\bar{\nu}_e$) is detected with $\bar{\nu}_e + p \rightarrow e^{+} + n$ (inverse beta decay)

Energy spectra of geoneutrinos

Nature 436, 28 July 2005

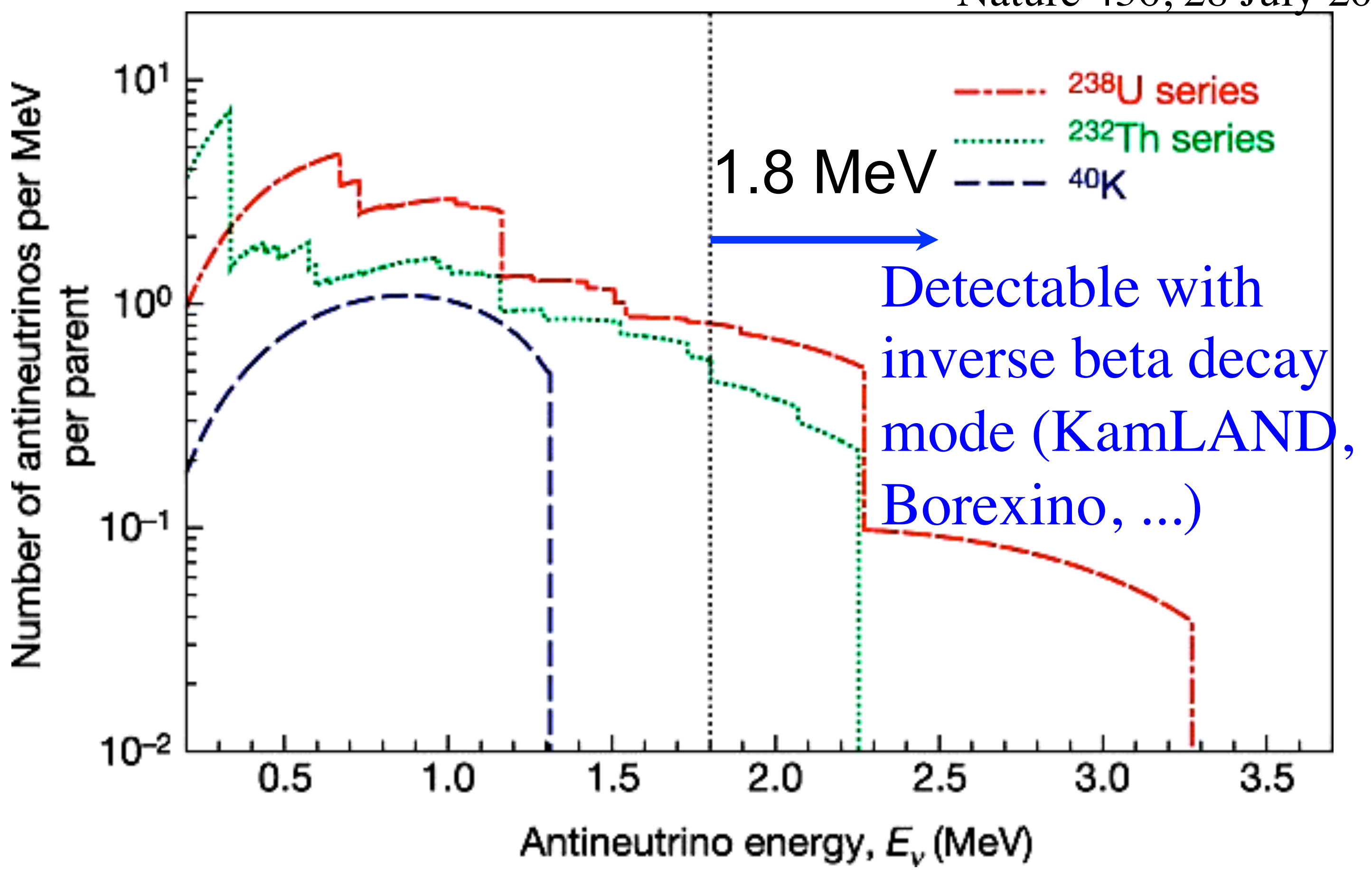

The expected ^{238}U, ^{232}Th, and ^{40}K decay chain electron anti-neutino energy distribution. KamLAND can only detect electron antineutrinos to the right of the vertical dotted black line; hence it is insensitive to ^{40}K electron antineutrinos.

Geoneutrino observation with KamLAND

Kamoka Liquid scintillator Antineutrino Detector

Japan, US, Europe collaboration lead by RCNS, Tohoku U.

Northern Japanese Alps

Gifu prefecture, Hida city, Kamioka mine
about 1000 m underground (2,700 m water equivalent) to avoid cosmic-ray background

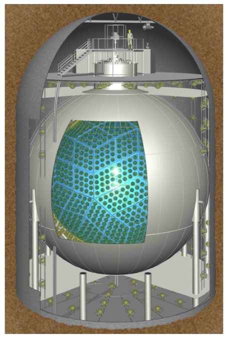

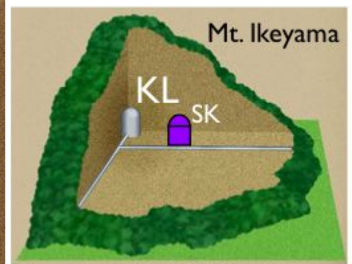

Geoneutrino flux at KamLAND site

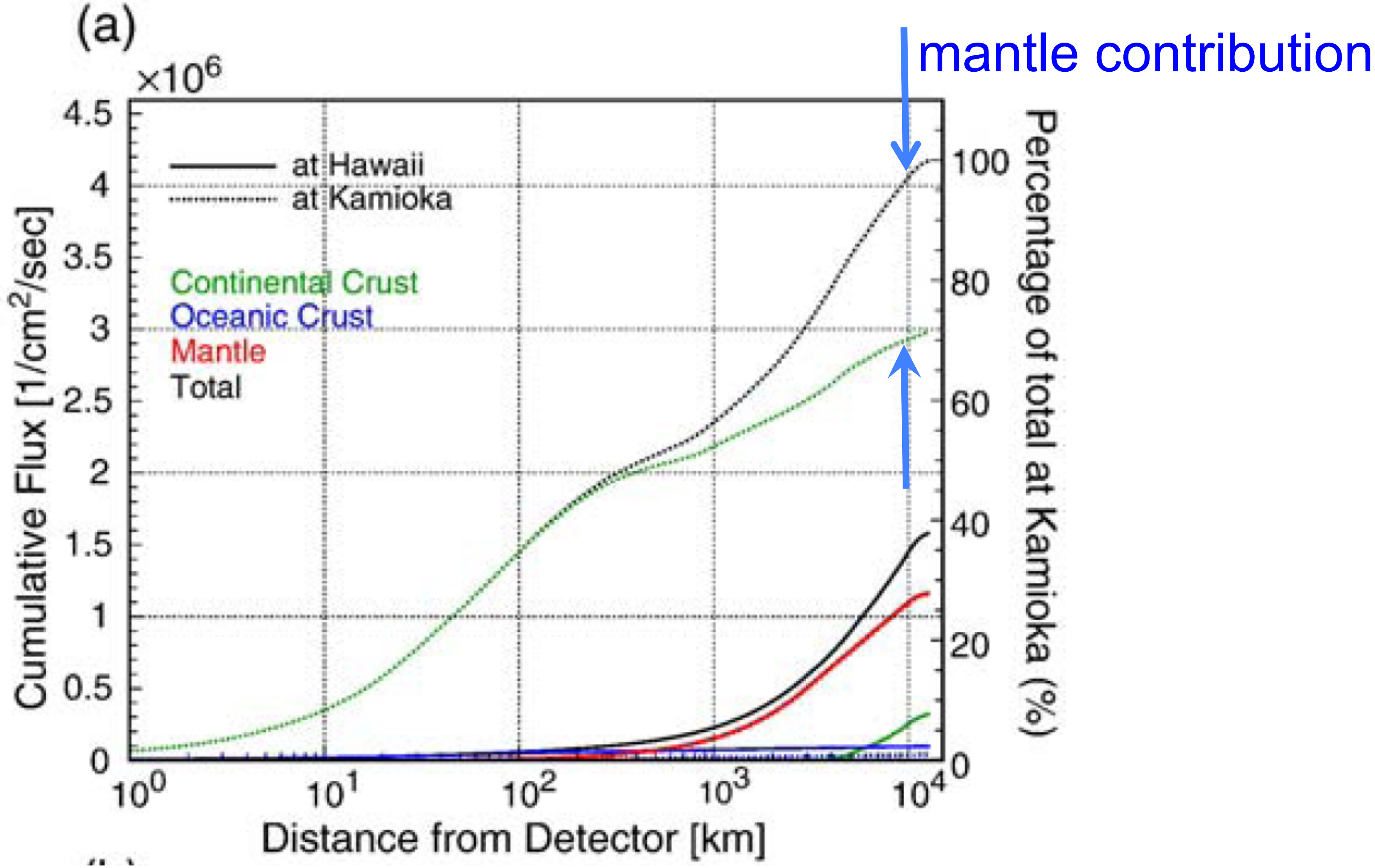

Reference model: S. Enomoto, E. Ohtani, KInoue, and A. Suzuki, Earth, Planet Sci. Lett. 258, 147 (2007)

KamLAND: 1000-ton ultrapure liquid scintillator

Inner Balloon installed in 2011

1879 phototubes cover 34% of the inner surface of the spherical stainless steel tank (18-m diameter)

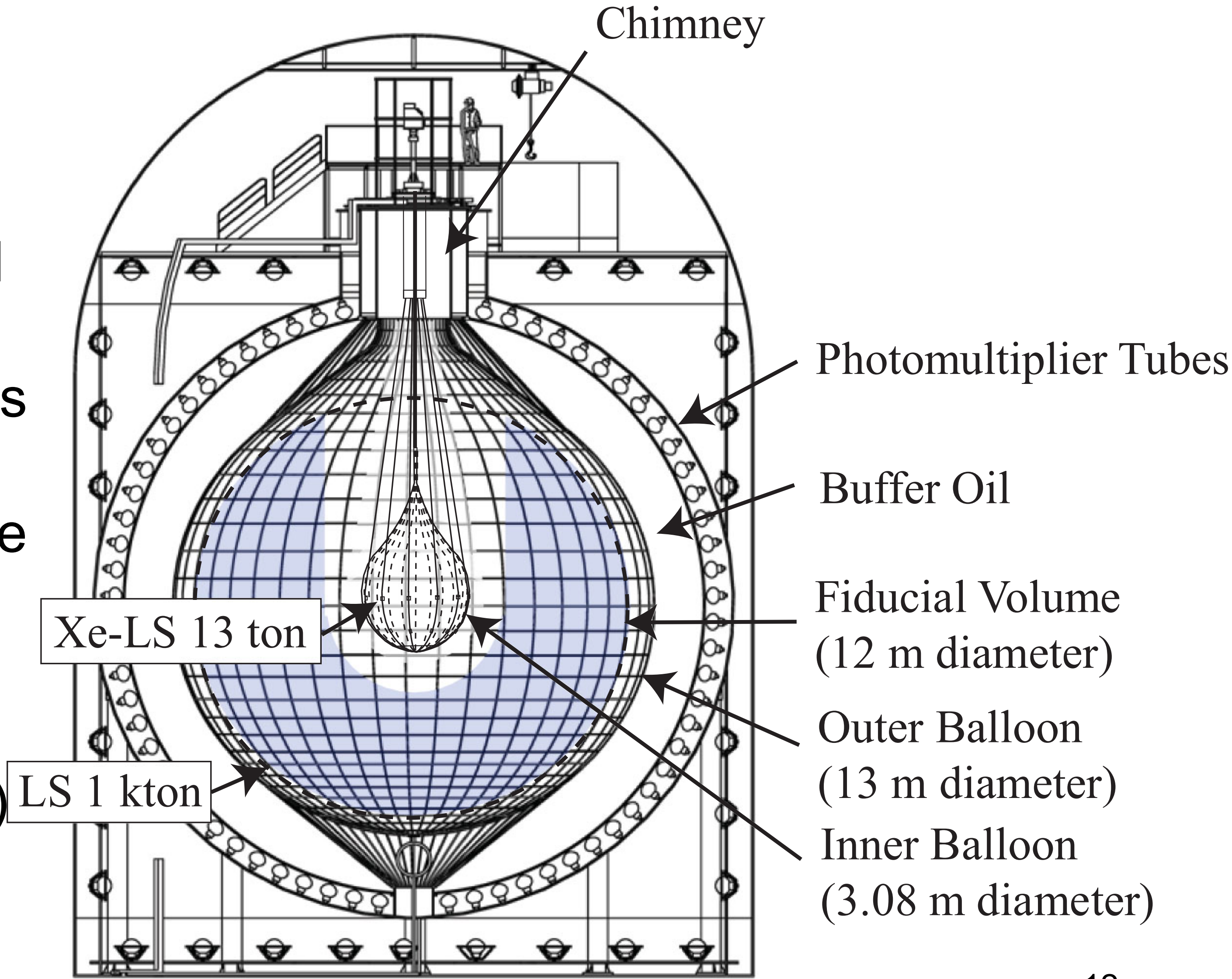

Kamioka Liquid *Antineutrino* Detector

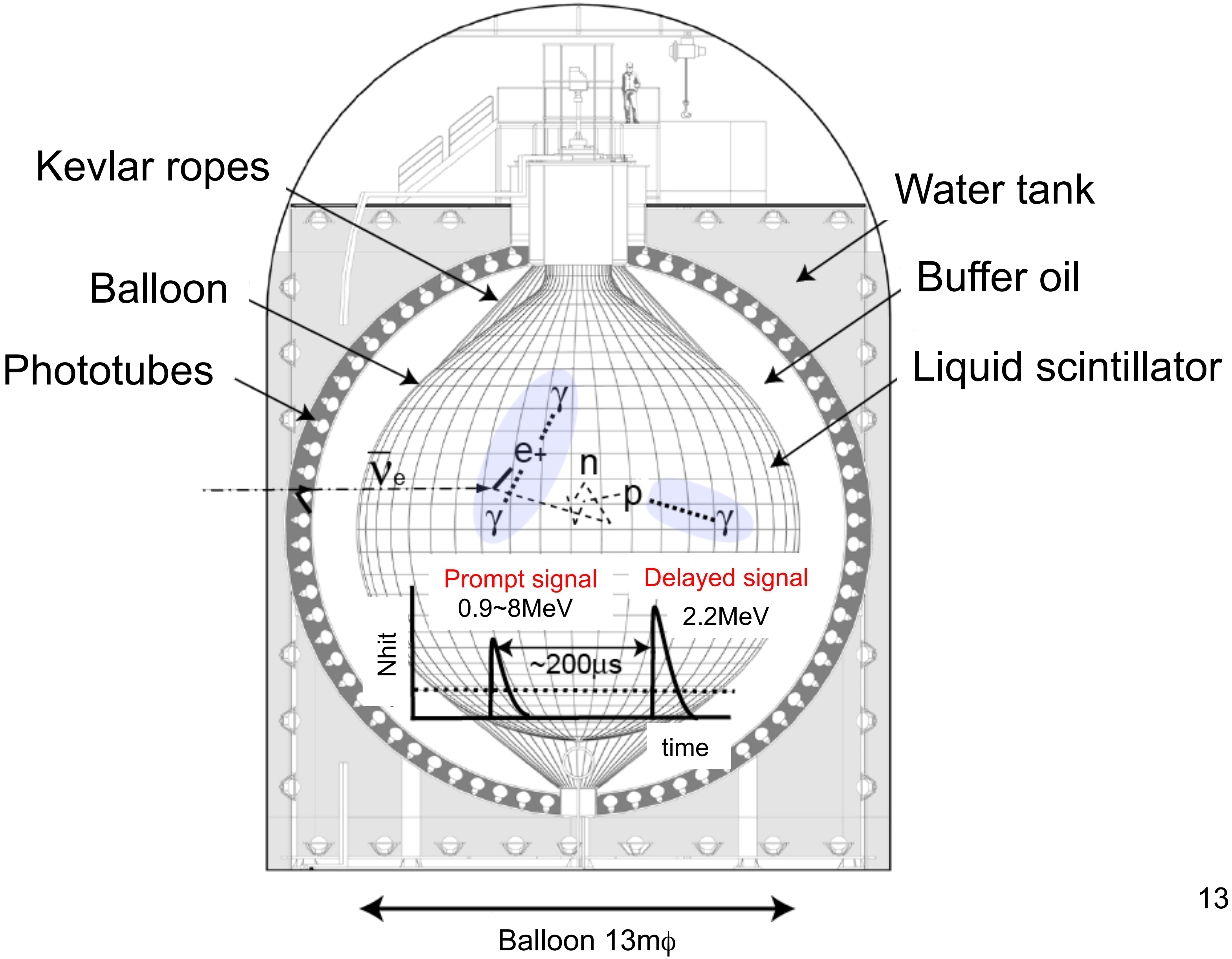

Contribution to the settlement of the solar neutrino problem (30-year problem)

Nuclear power reactors

The settlement was an important breakthrough, and should be basics of all fluxes measurement with Borexino.

Sun

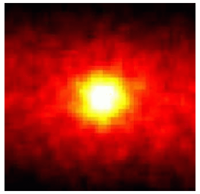

(*1)

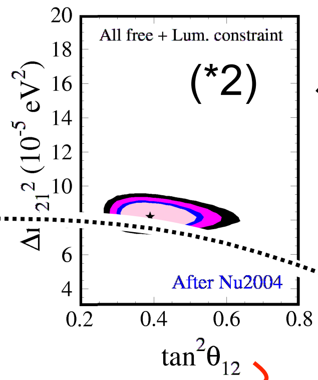

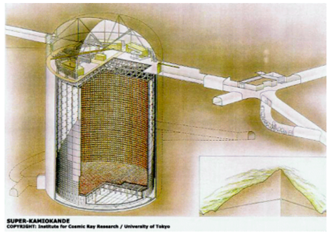

Super-Kamiokande

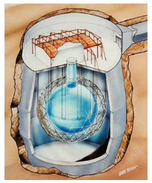

SNO

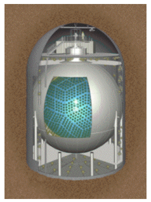

KamLAND

Solar neutrino deficit (1970's)
Solar or neutrino problem? (30 years)
Settlement (2002) with neutrino oscillation

(*1) neutrinograph of the sun by Super-K, (*2) hep-ph/0406294

First result from KamLAND (2002)

PRL **90**, 021802 Dec. 2002

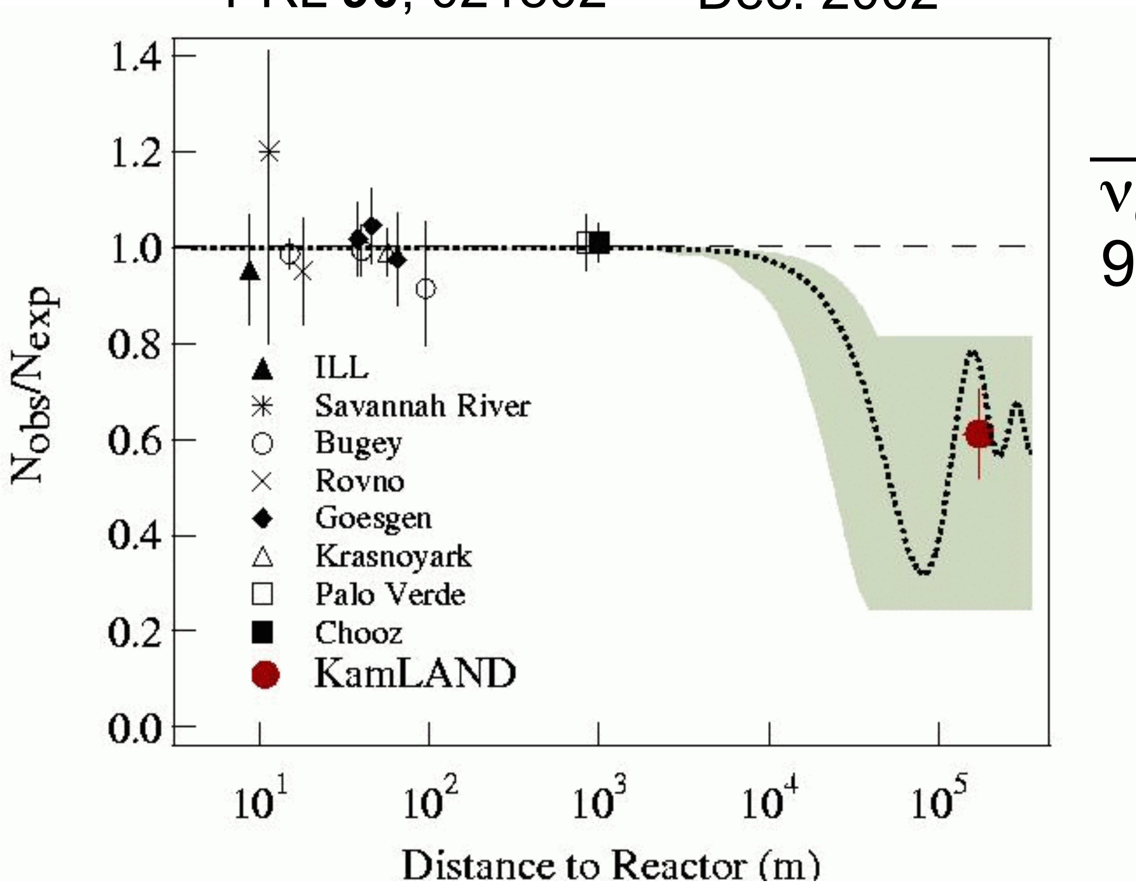

$\bar{\nu}_e$ disappearance:
99.95 % C.L.

Geoneutrino first results in 2005

152 events observed

“signal” 25 $^{+19}_{-18}$

Nature 436, 28 July 2005

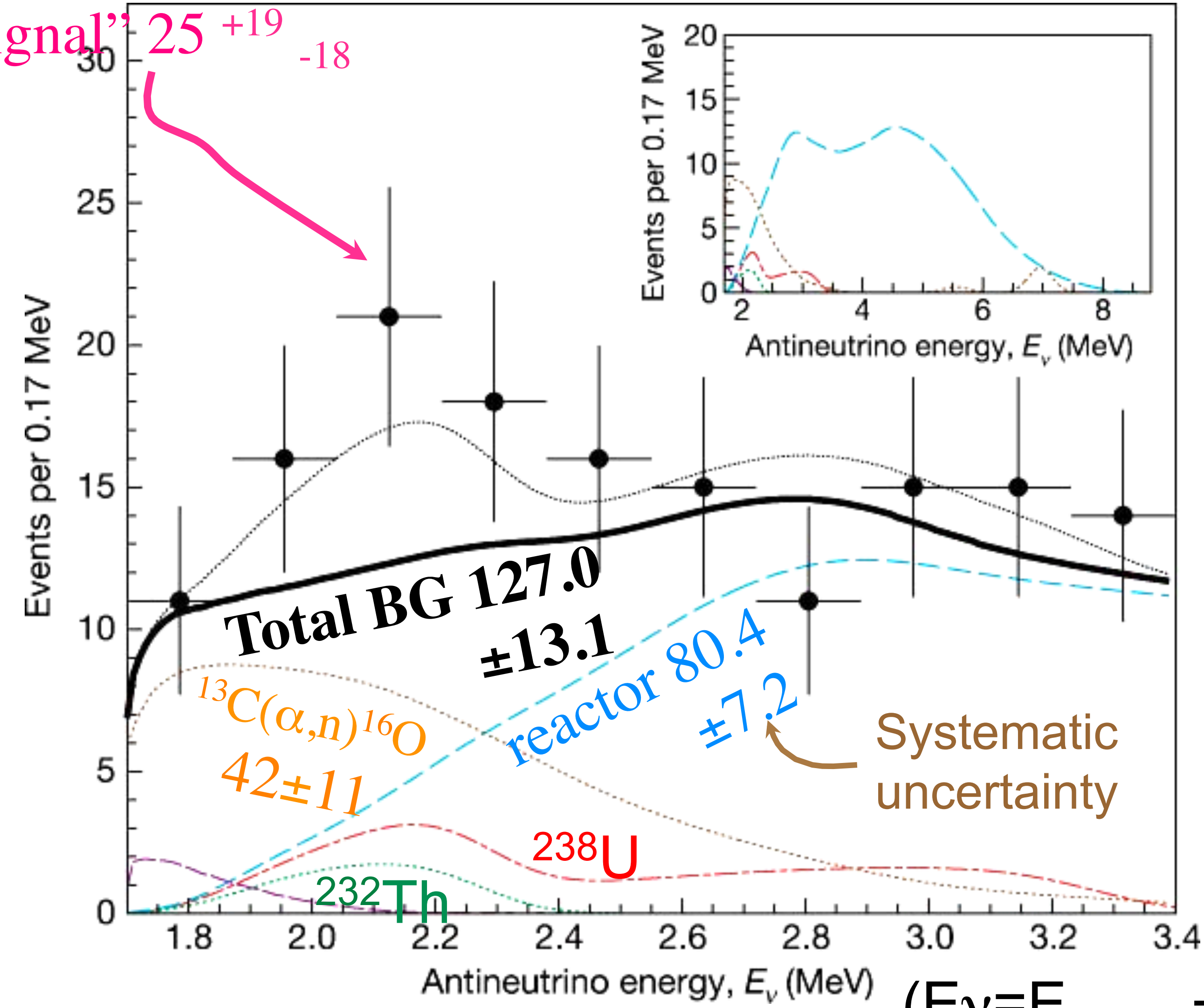

Data-set:

749.1 days

(Mar. 9, 2002 -Oct. 30, 2004)

Fiducial:

5 m radius

($E\nu = E_{prompt}$+0.8MeV)

Geoneutrino observation with KamLAND (the latest published data (2013)

Data set

- ``Reactor on-off antineutrino measurement with KamLAND'', Phys. Rev. D 88 033001 (2, August, 2013)
- March 9, 2002 – November 20, 2012

  (2991 days live-time)
- Data set is divided into 3 period

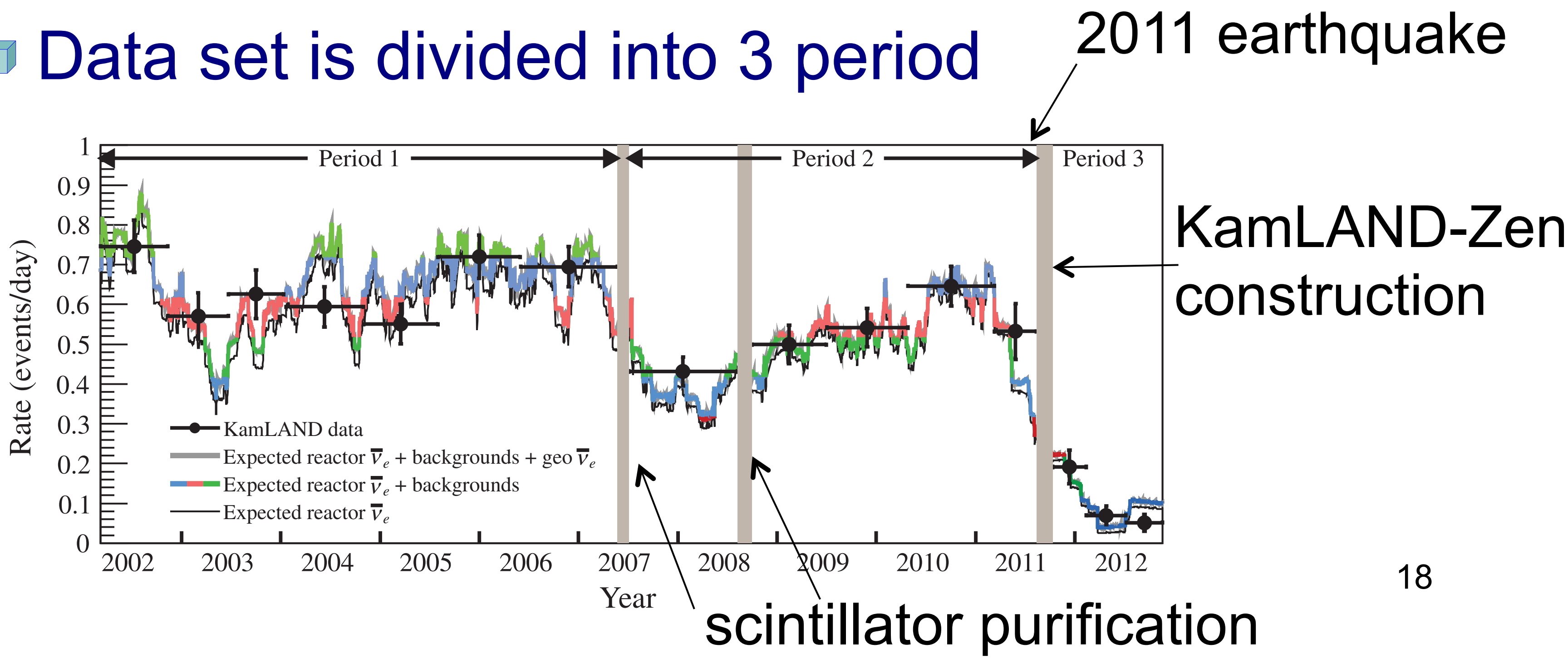

Energy calibration

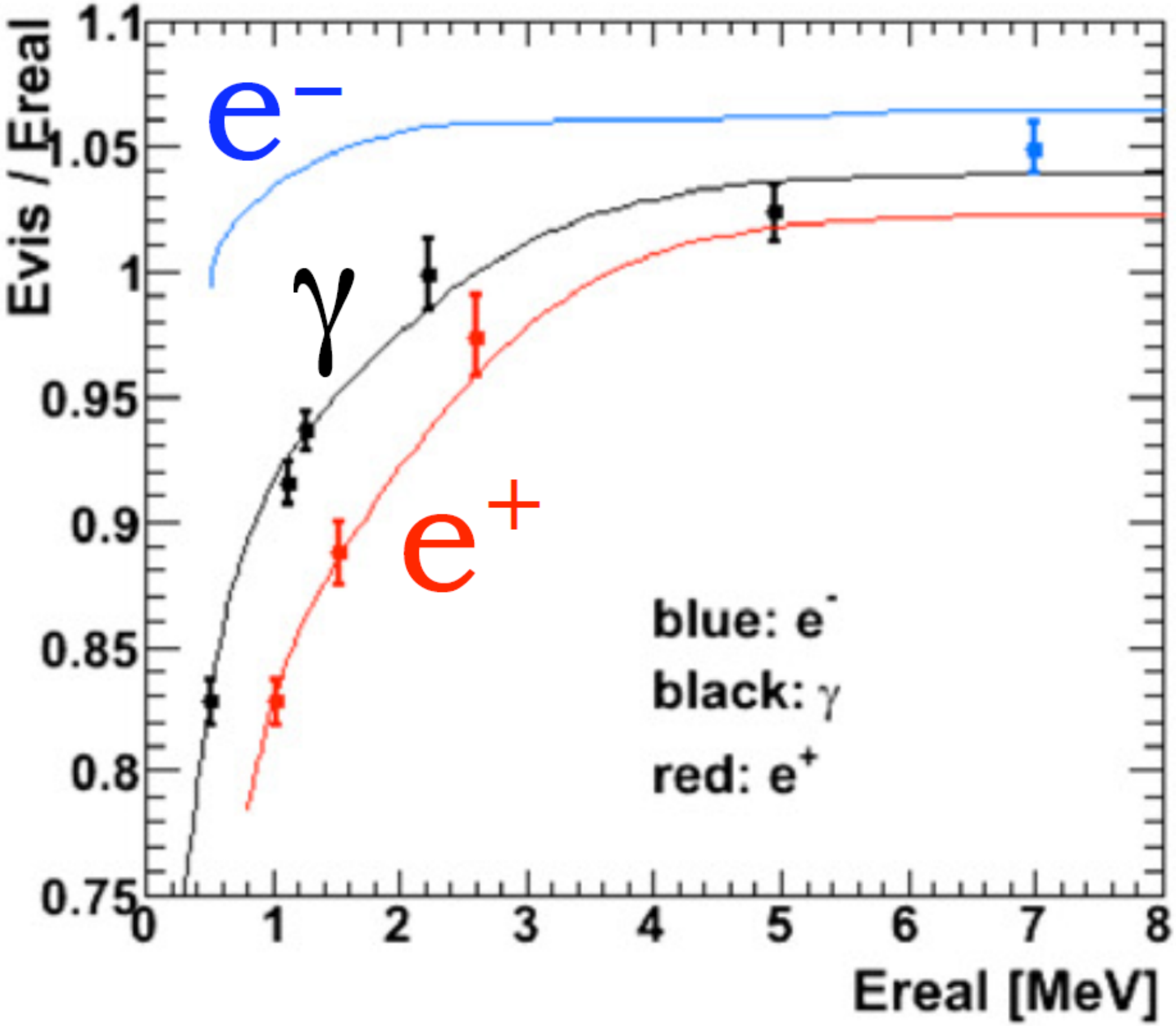

Cherenkov-Birks model

Data reduction (event selection)

- Fiducial volume (event within which is considered available): R < 6 m (mini balloon cut for period 3)
- Delayed coincidence:
  - Prompt energy: 0.9 – 8.5 MeV
  - (neutrino energy: 1.7 – 9.3 MeV)
  - Delayed energy: 1.8 – 2.6 MeV, or 4.4 – 5.6 MeV
  - (peak at 2.2 MeV, and 4.9 MeV)
  - Spatial correlation: < 2.0 m
  - Time correlation: 0.5 – 1000 μs
- Additional selection to suppress accidental coincidence further, based on probability densities of accidental coincidence and real signal

Kamioka Liquid *Antineutrino* Detector

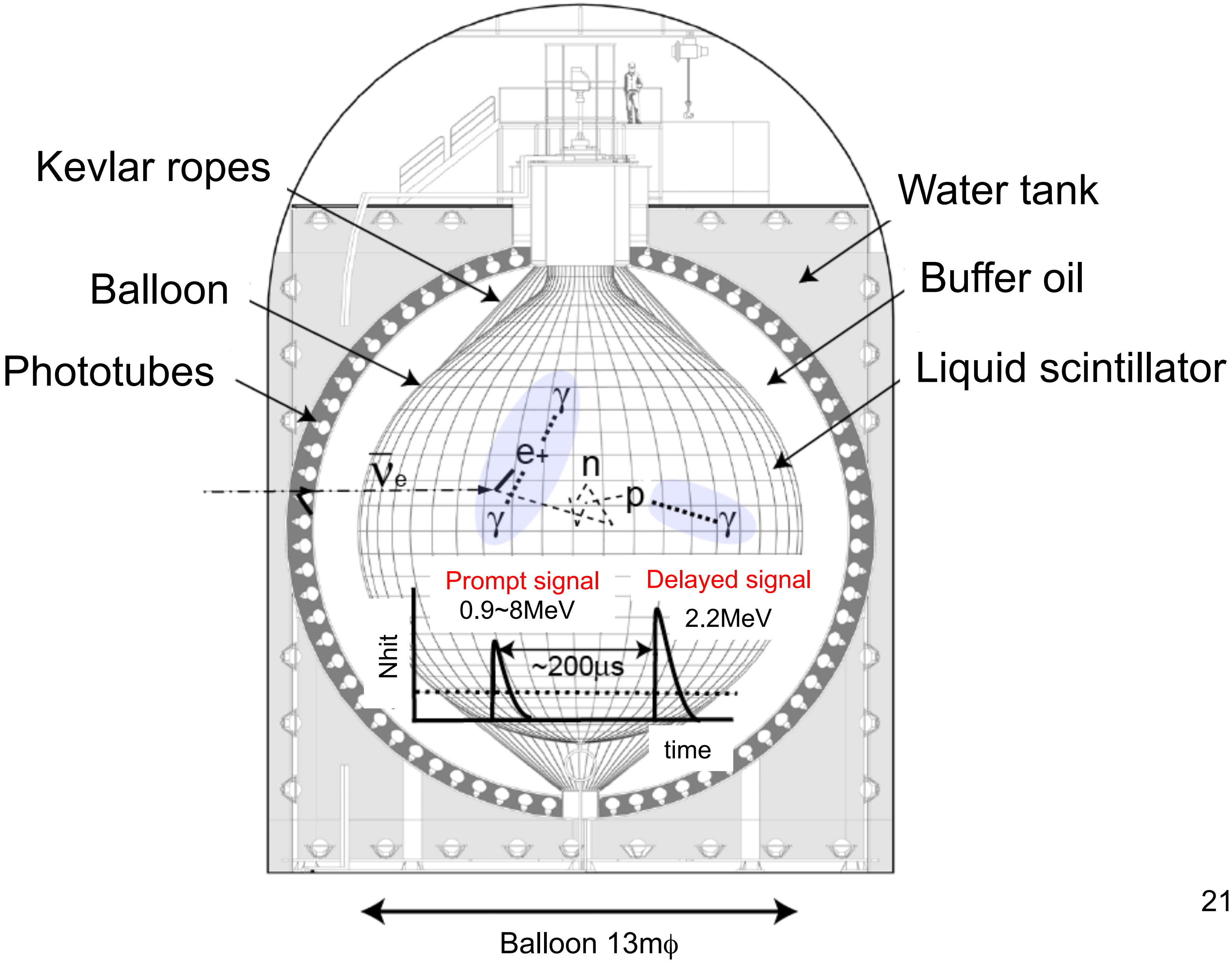

Prompt energy (neutrino energy – 1.8 MeV) spectrum: all period

- $116\ ^{+28}_{-27}$ geoneutrino events are detected (U/Th = 3.9 fixed, energy spectrum, time variation included, unbinned, all 3 periods)
- U: 116 events
- Th: 8 events

with U, Th free fitting

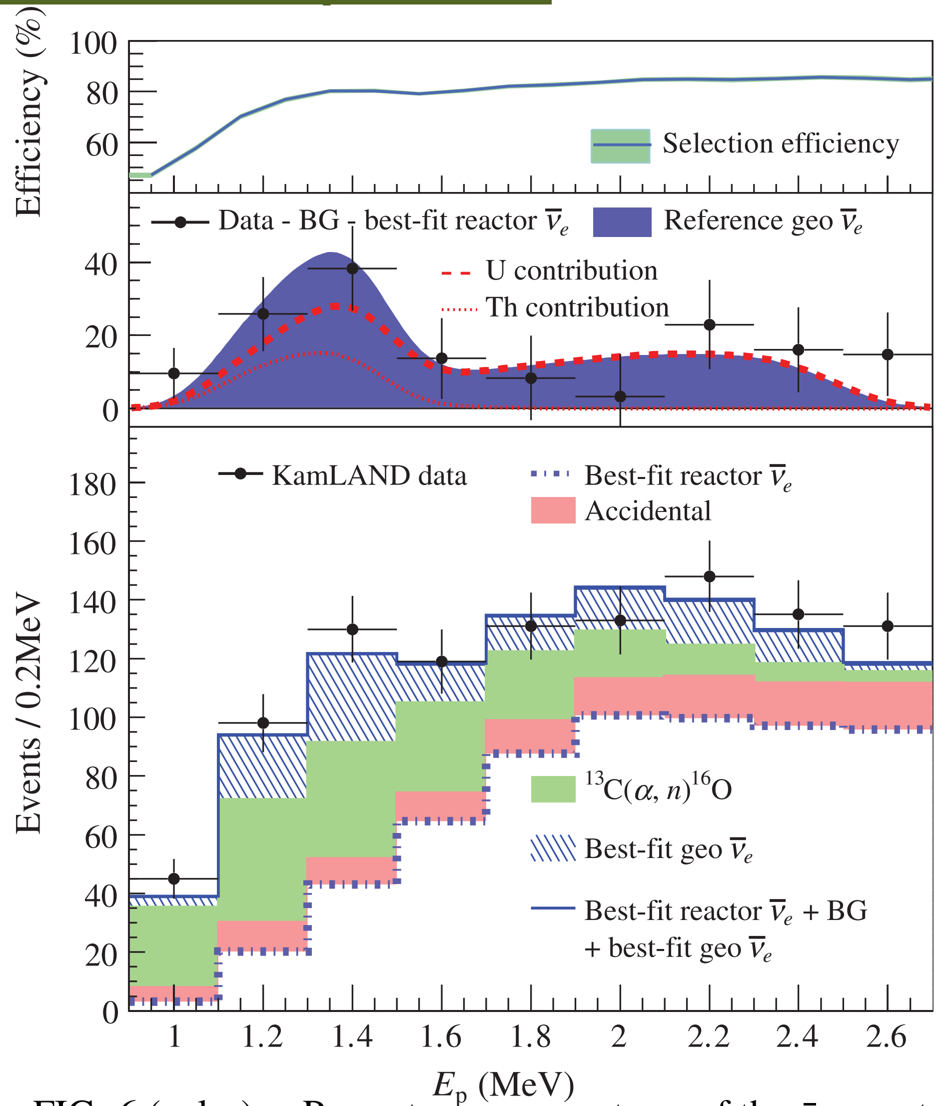

FIG. 6 (color). Prompt energy spectrum of the $\bar{\nu}_e$ events in the low-energy region for all data-taking periods. Bottom panel:

Energy spectrum of each period

- $^{13}C(\alpha,n)^{16}O$ background is reduced by a factor of 20 in Period 2. (by scintillator purification)
- Reactor background decreased in Period 3

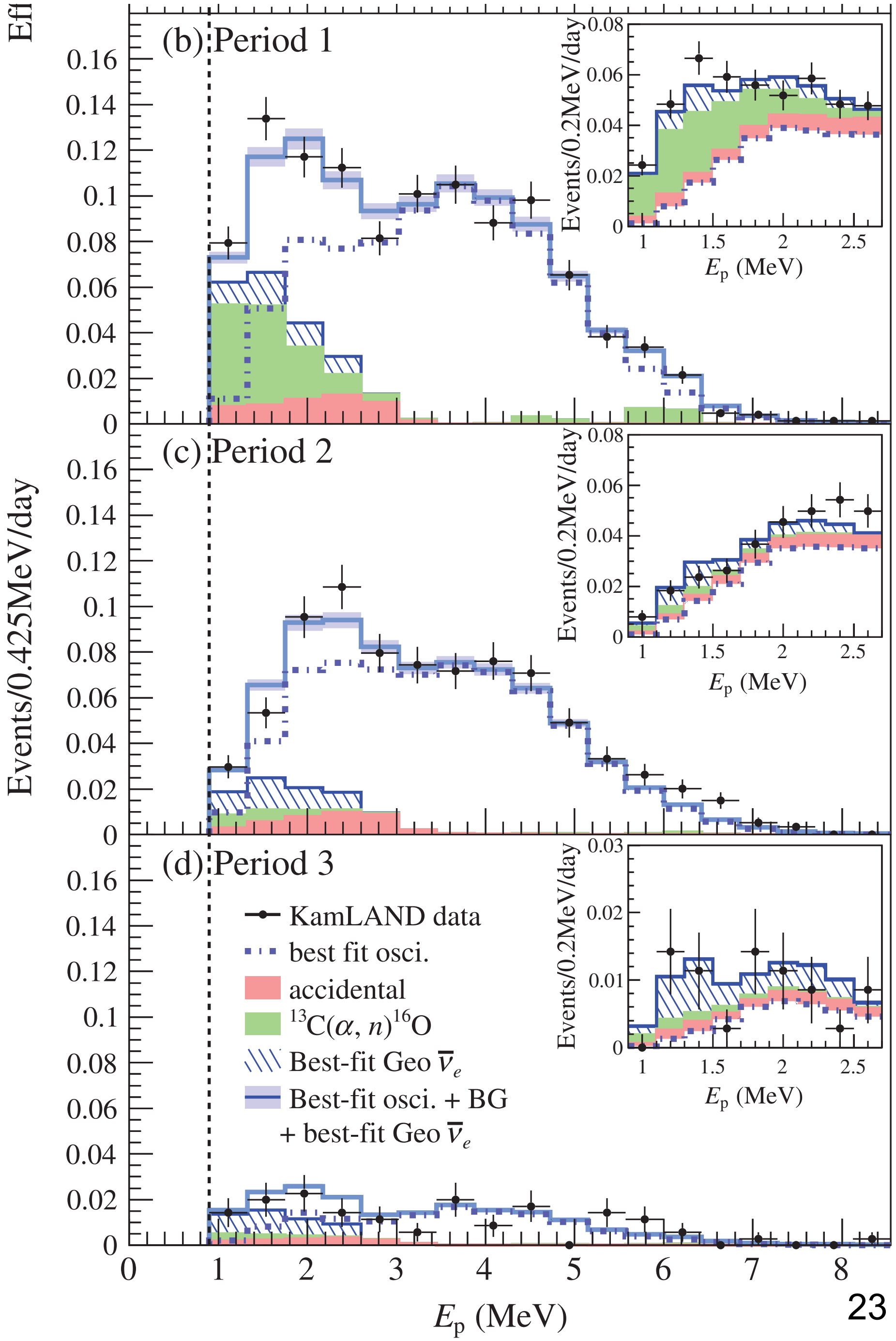

Time variation: 0.9 – 2.6 MeV (geoneutrino region)

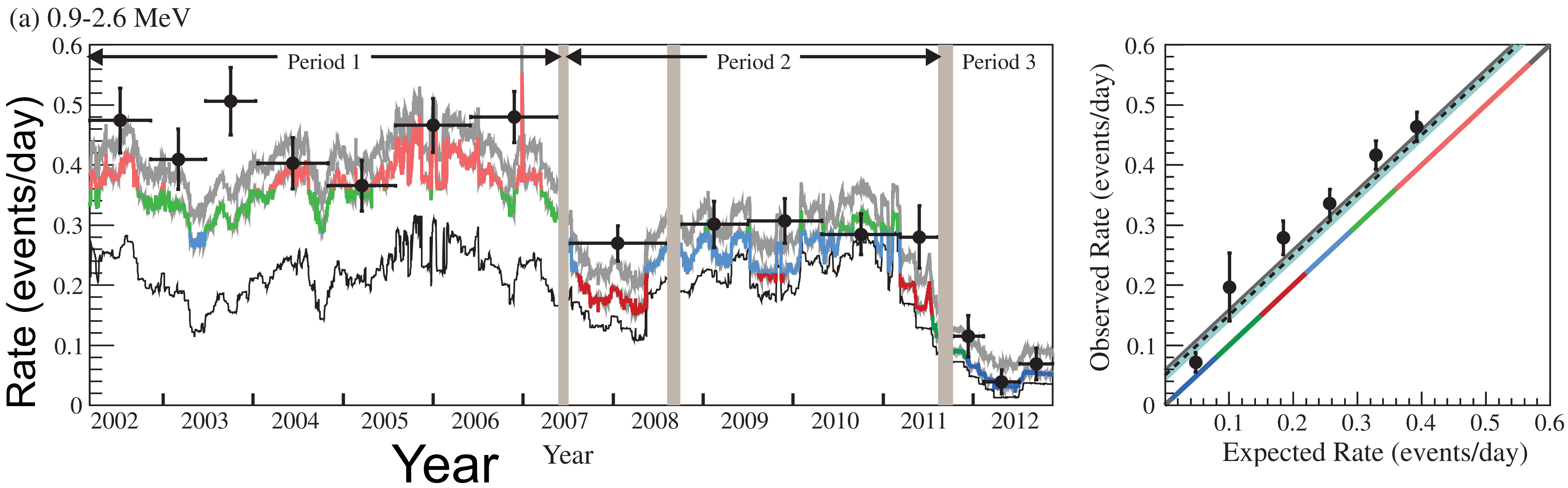

- Data (solid circles) and expected rate (reactor + b.g. + geo, grey curve) are consistent, not consistent with reactor + b.g. only (colored curve)
- Data are on the unit slope with finite displacement, indicating constant contribution from geoneutrinos!

Time variation: 0.9 – 2.6 MeV (geoneutrino region)

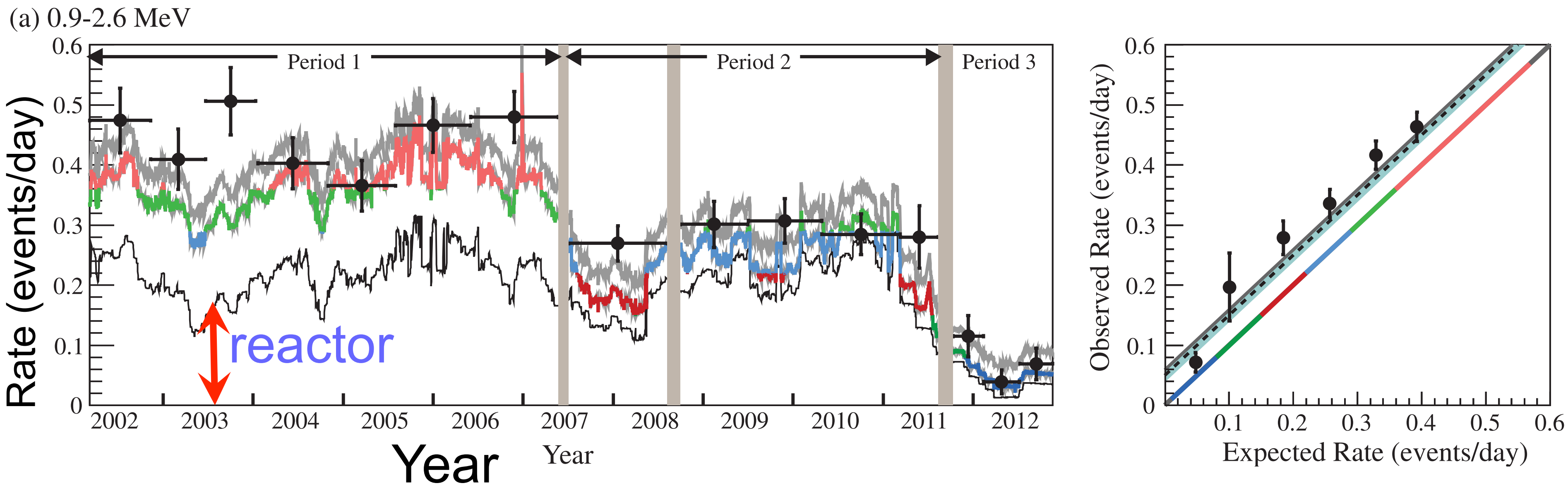

- Data (solid circles) and expected rate (reactor + b.g. + geo, grey curve) are consistent, not consistent with reactor + b.g. only (colored curve)
- Data are on the unit slope with finite displacement, indicating constant contribution from geoneutrinos!

Time variation: 0.9 – 2.6 MeV (geoneutrino region)

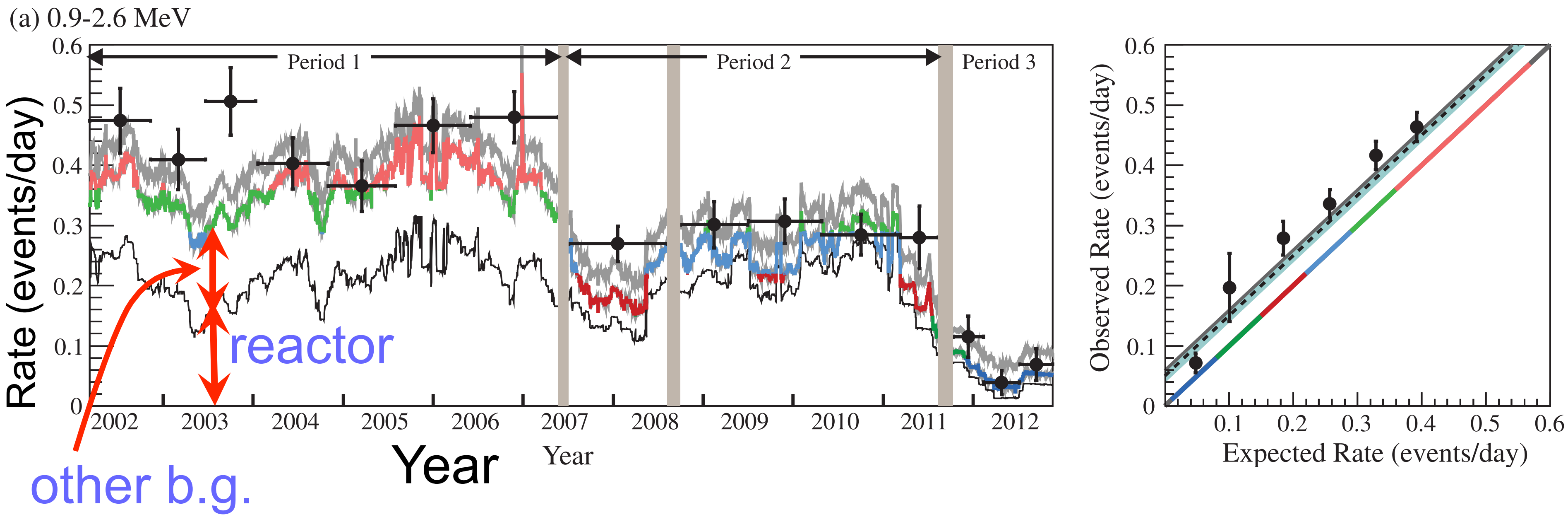

- Data (solid circles) and expected rate (reactor + b.g. + geo, grey curve) are consistent, not consistent with reactor + b.g. only (colored curve)
- Data are on the unit slope with finite displacement, indicating constant contribution from geoneutrinos!

Time variation: 0.9 – 2.6 MeV (geoneutrino region)

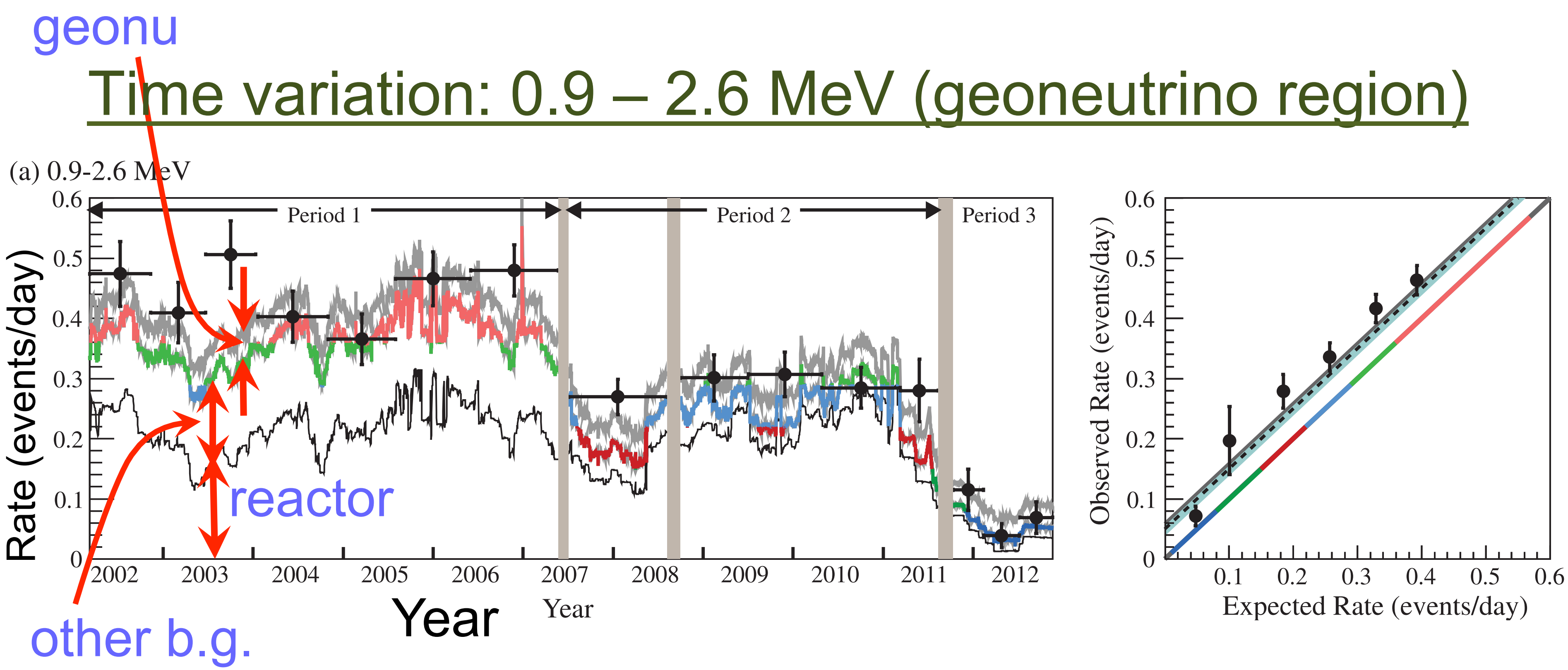

- Data (solid circles) and expected rate (reactor + b.g. + geo, grey curve) are consistent, not consistent with reactor + b.g. only (colored curve)
- Data are on the unit slope with finite displacement, indicating constant contribution from geoneutrinos!

Time variation: 0.9 – 2.6 MeV (geoneutrino region)

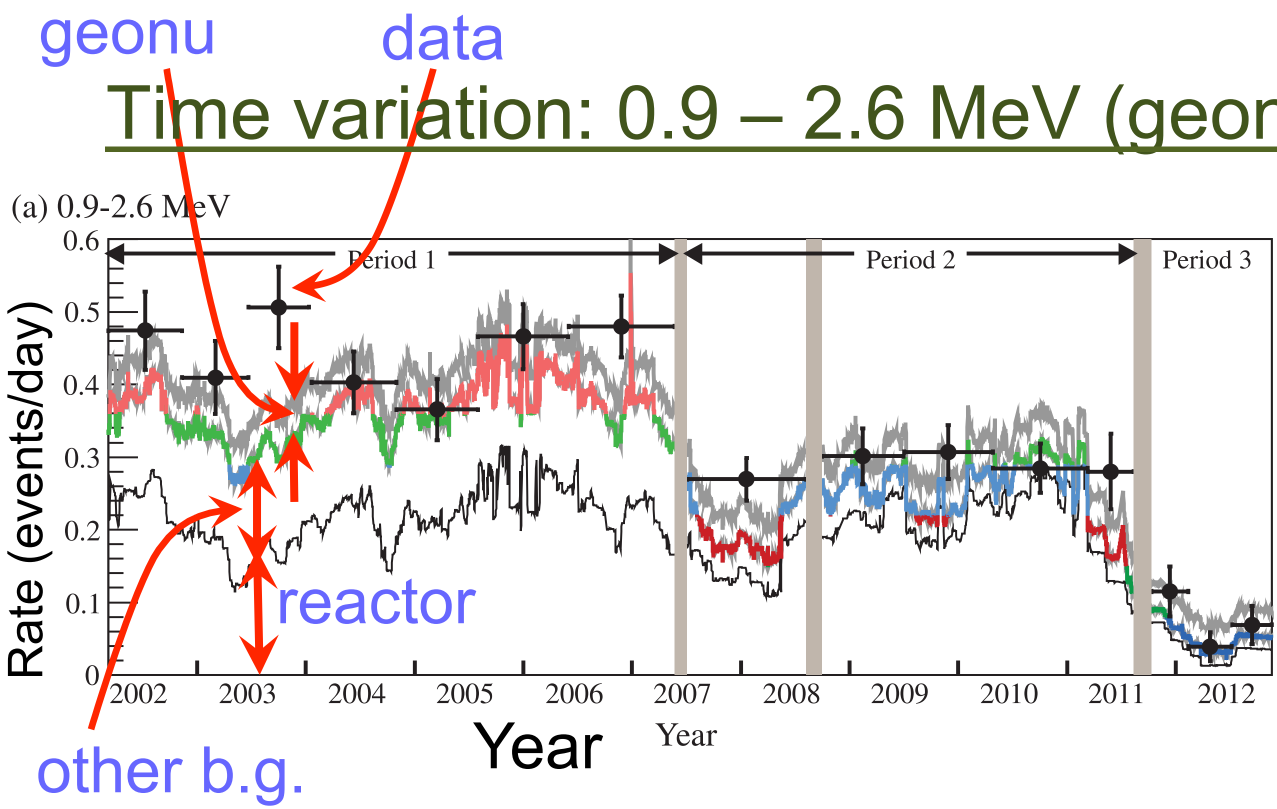

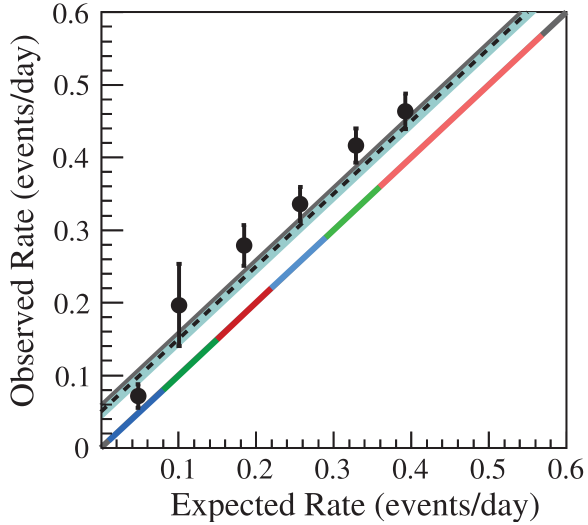

- Data (solid circles) and expected rate (reactor + b.g. + geo, grey curve) are consistent, not consistent with reactor + b.g. only (colored curve)
- Data are on the unit slope with finite displacement, indicating constant contribution from geoneutrinos!

Time variation: 0.9 – 2.6 MeV (geoneutrino region)

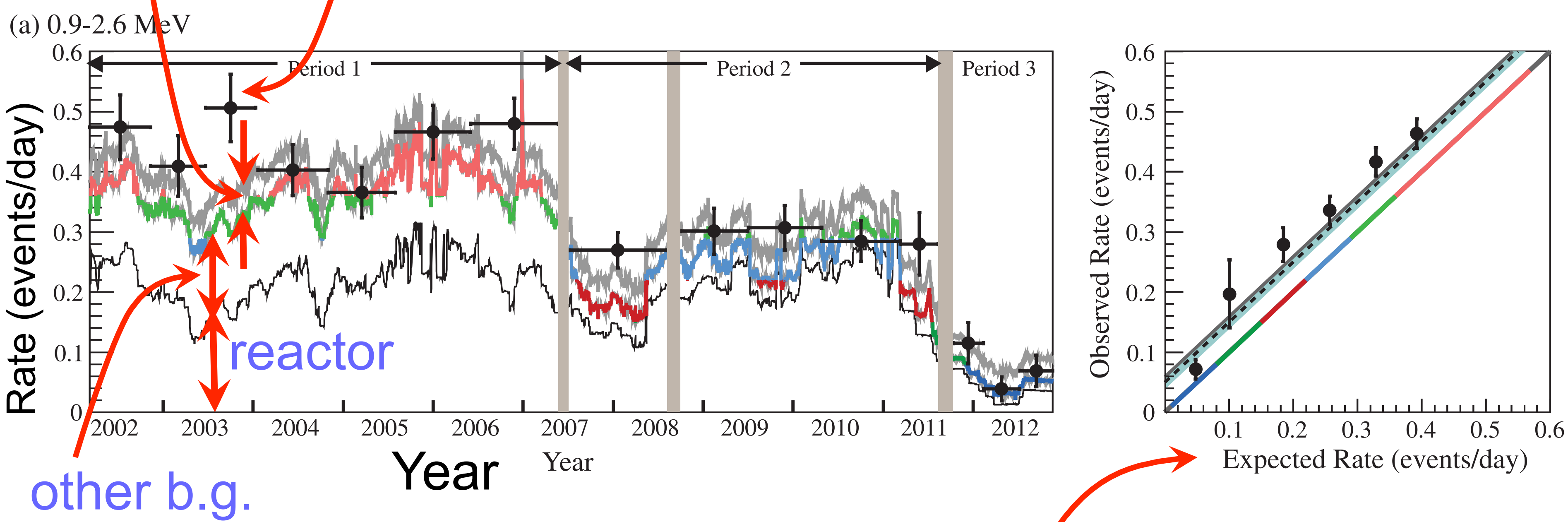

- Data (solid circles) and expected rate (reactor + b.g. + geo, grey curve) are consistent, not consistent with reactor + b.g. only (colored curve)
- Data are on the unit slope with finite displacement, indicating constant contribution from geoneutrinos!

Expected Rate of reactor + other b.g. (without geonu)

Time variation: 2.6 – 8.5 MeV (reactor region)

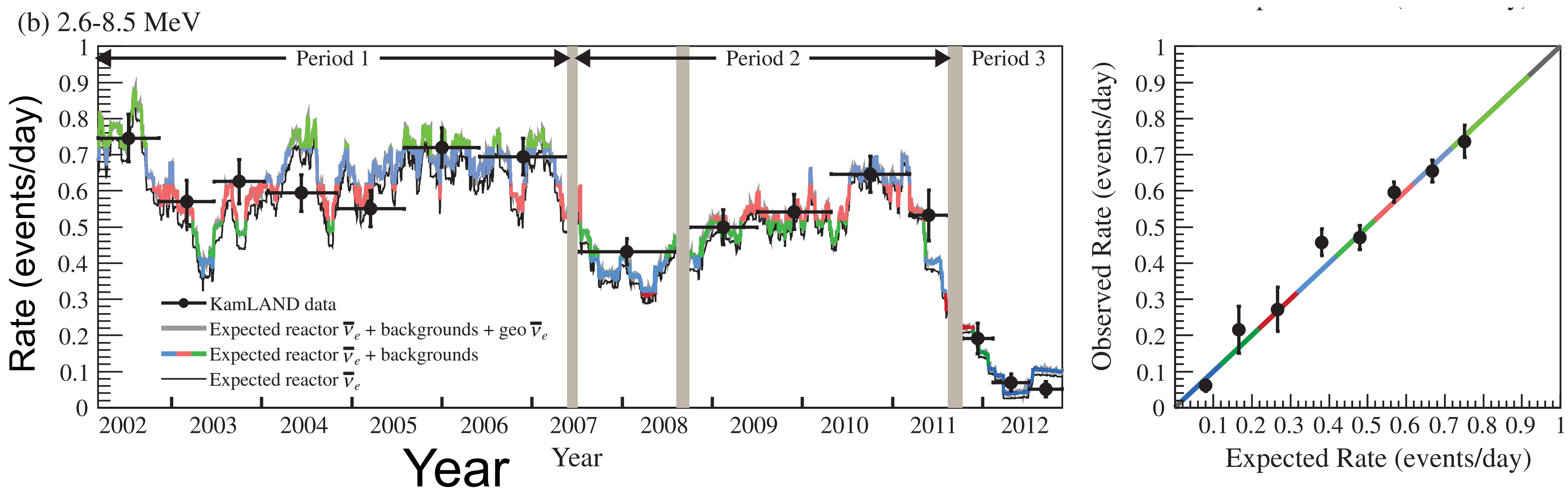

- Data (solid circles) and expected rate (reactor + b.g. + geo, grey curve) are consistent
- Data are on the unit slope with zero displacement (right panel): quite consistent again!

Time variation (reactor and geo regions)

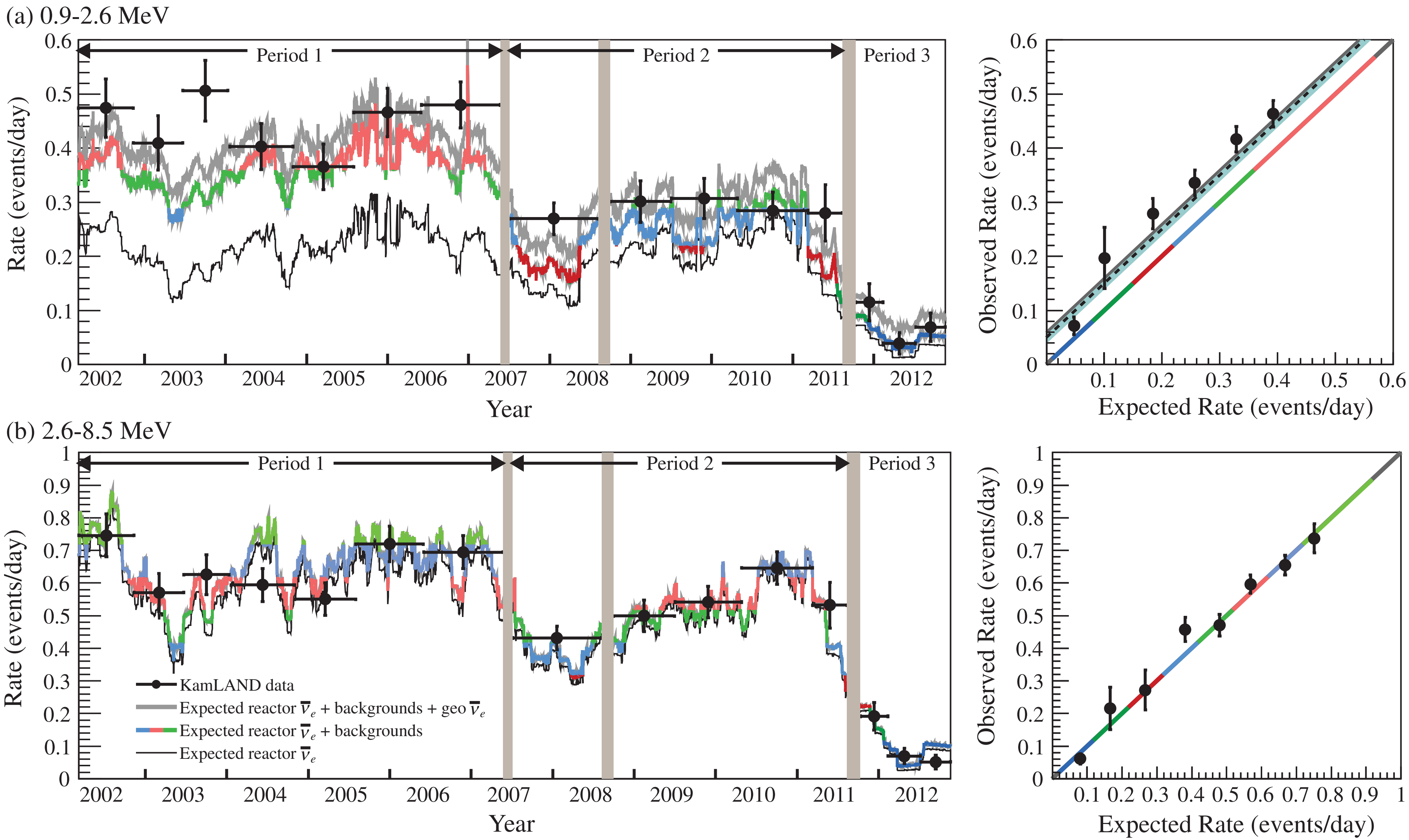

Comparison with the reference model

- U, Th event rates are consistent with the reference model
- With fixed Th/U = 3.9, total geoneutrino events are 116^{+28}_{-27}, excluding no geoneutrino hypothesis with more than 4 sigma
- Uranium neutrino positive: Th/U < 19 (90% C.L.)

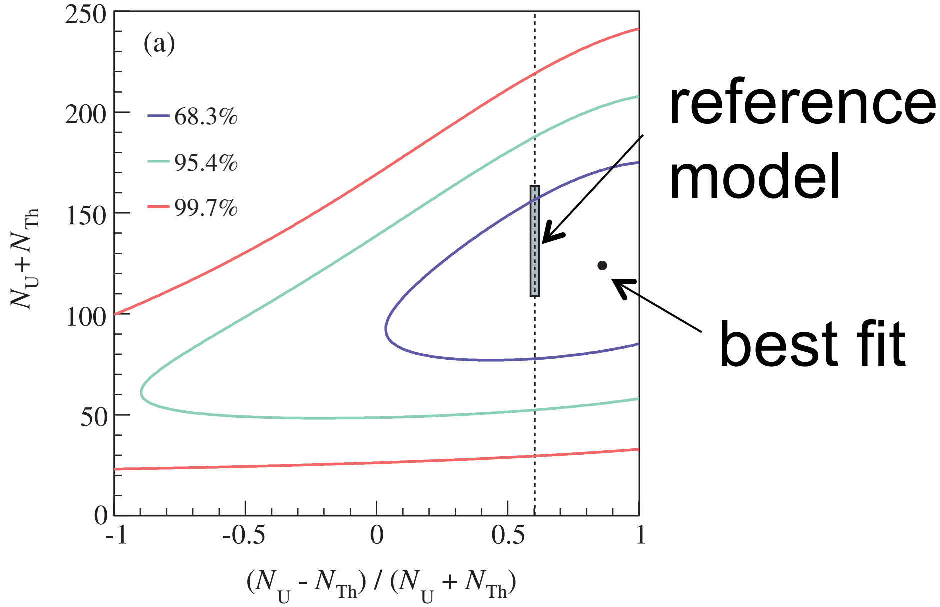

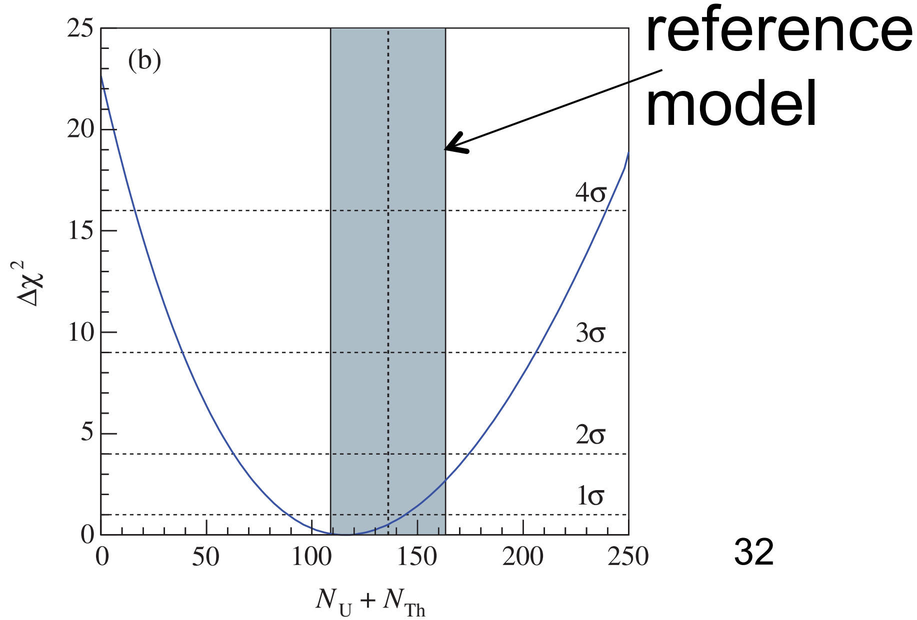

Partially radiogenic heat of the Earth

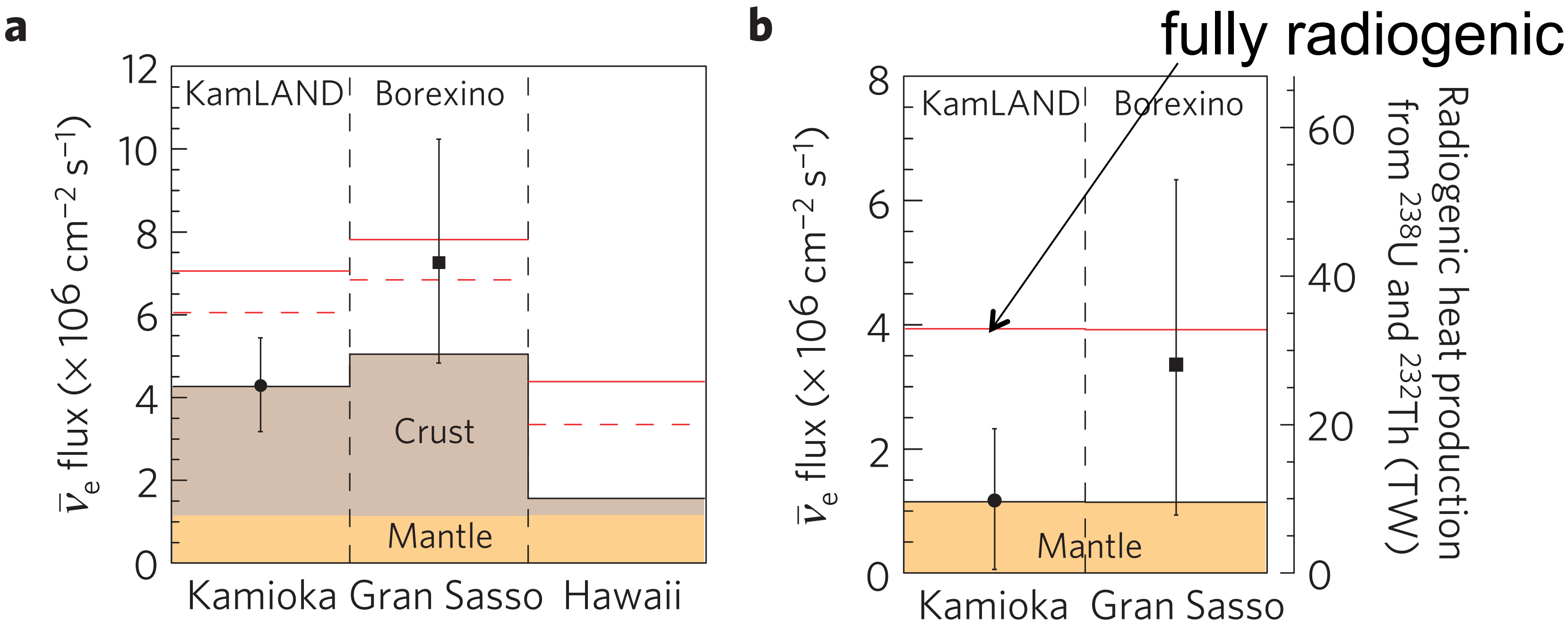

``Partial radiogenic heat model for Earth revealed by geoneutrino measurements'', Nature Geoscience 17, July 2011
(only this figure is from our previous publication that does not include low reactor period after 2011)

- Fully radiogenic model (homogeneous mantle) is excluded with 98 % C.L. (total heat flow 46±3 TW (Jaupart et al. 2007) assumed)

Comparison with other models

- ``convective Urey ratio'' (radiogenic heat source in the mantle) / (total heat source): 0.09 – 0.42 (68 % C.L.)
  → consistent with BSE model (0.3), primordial heat source necessary
- Geodynamical model that assumes relatively high Urey ratio, is becoming to be disfavored

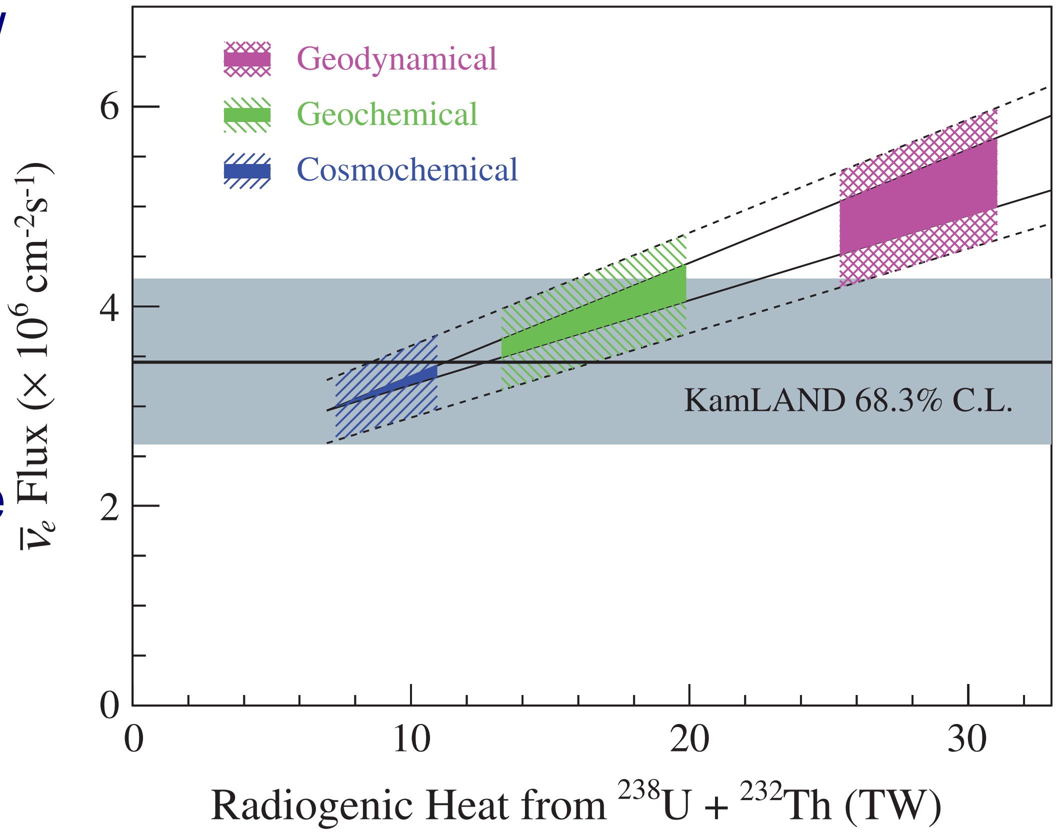

Geoneutrino observation with Borexino

PHYS. REV. D 101, 012009 (2020)

"Comprehensive Geoneutrino Analysis with Borexino"
(really comprehensive. All geoneutrino researchers are recommended to read this original paper)

Borexino detector

- Laboratori Nazionali del Gran Sasso LNGS (Italy)
- 3800 m.w.e
- Far away from reactors ~ 1200 km
- Ultrapure liquid scintillator

  (so pure as to measure all fluxes of solar neutrinos)

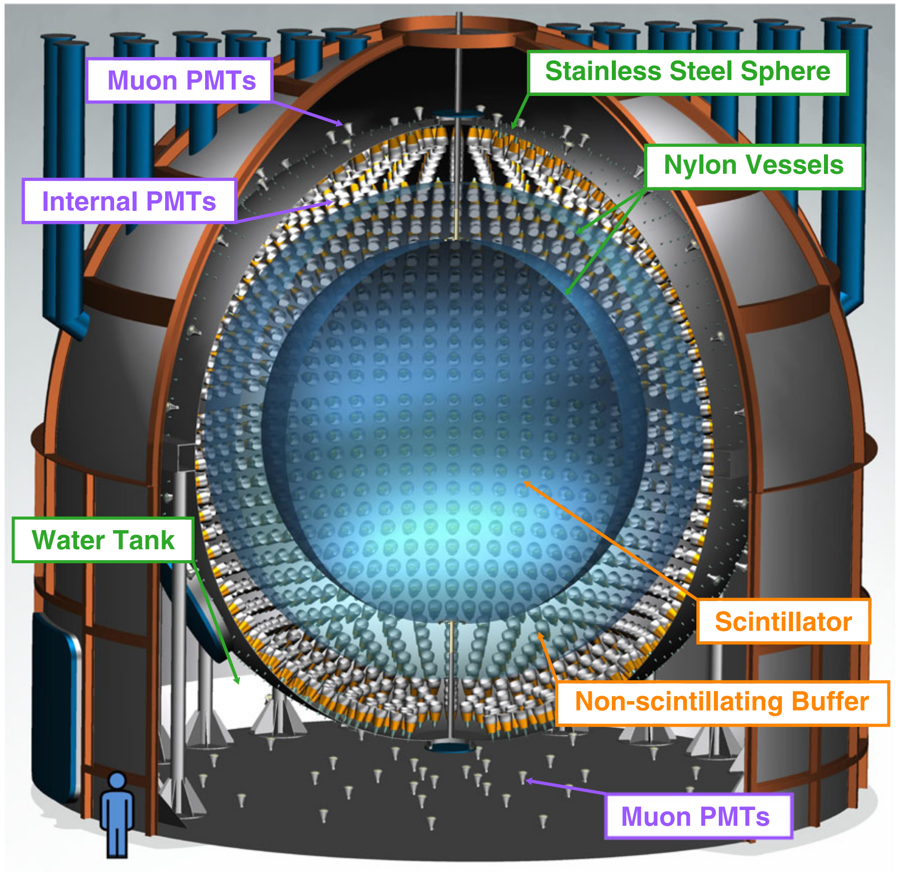

FIG. 2. Scheme of the Borexino detector.

PHYS. REV. D 101, 012009 (2020)

Particle ID (α v.s. β/γ)

- Particle identification (ID) using pulse shape (time profile) difference of scintillation light has been improved

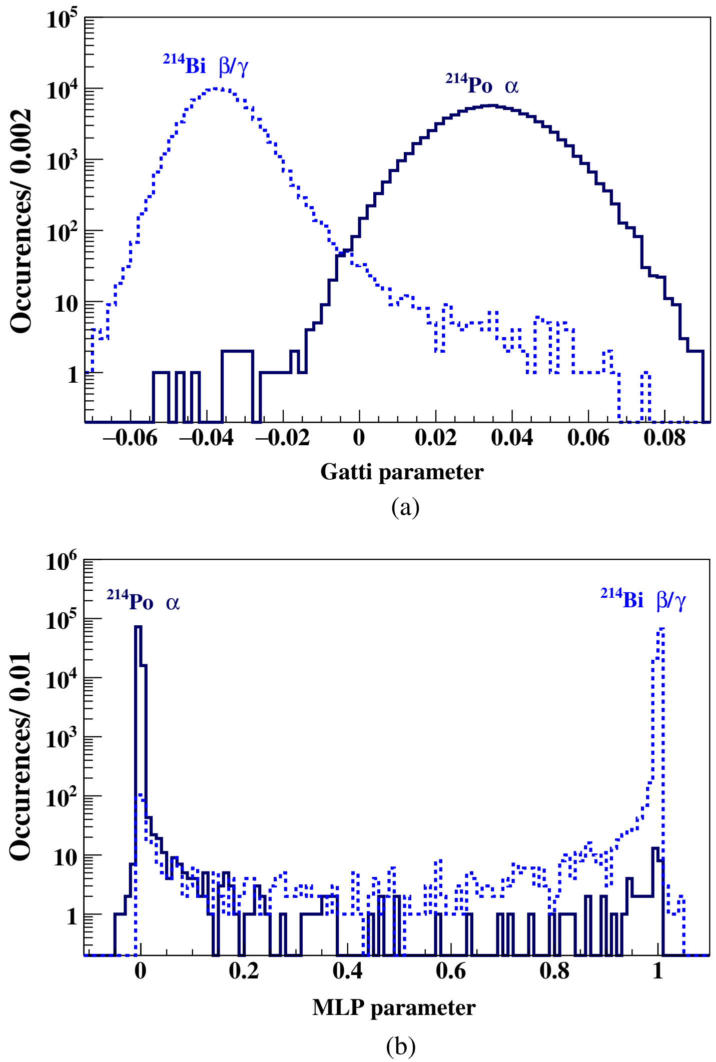

FIG. 11. Distributions of the Gatti (G) (a) and the multilayer perceptron (MLP) (b) α/β discrimination parameters for ^{214}Bi(β^-) (dashed line) and ^{214}Po(α) (solid line) events.

PHYS. REV. D 101, 012009 (2020)

Results

- energy spectra of IBD (inverse beta decay) events (electron antineutrino events)
- Geoneutrino measurement achieved
- analyses with Th/U ratio fixed and free agreed

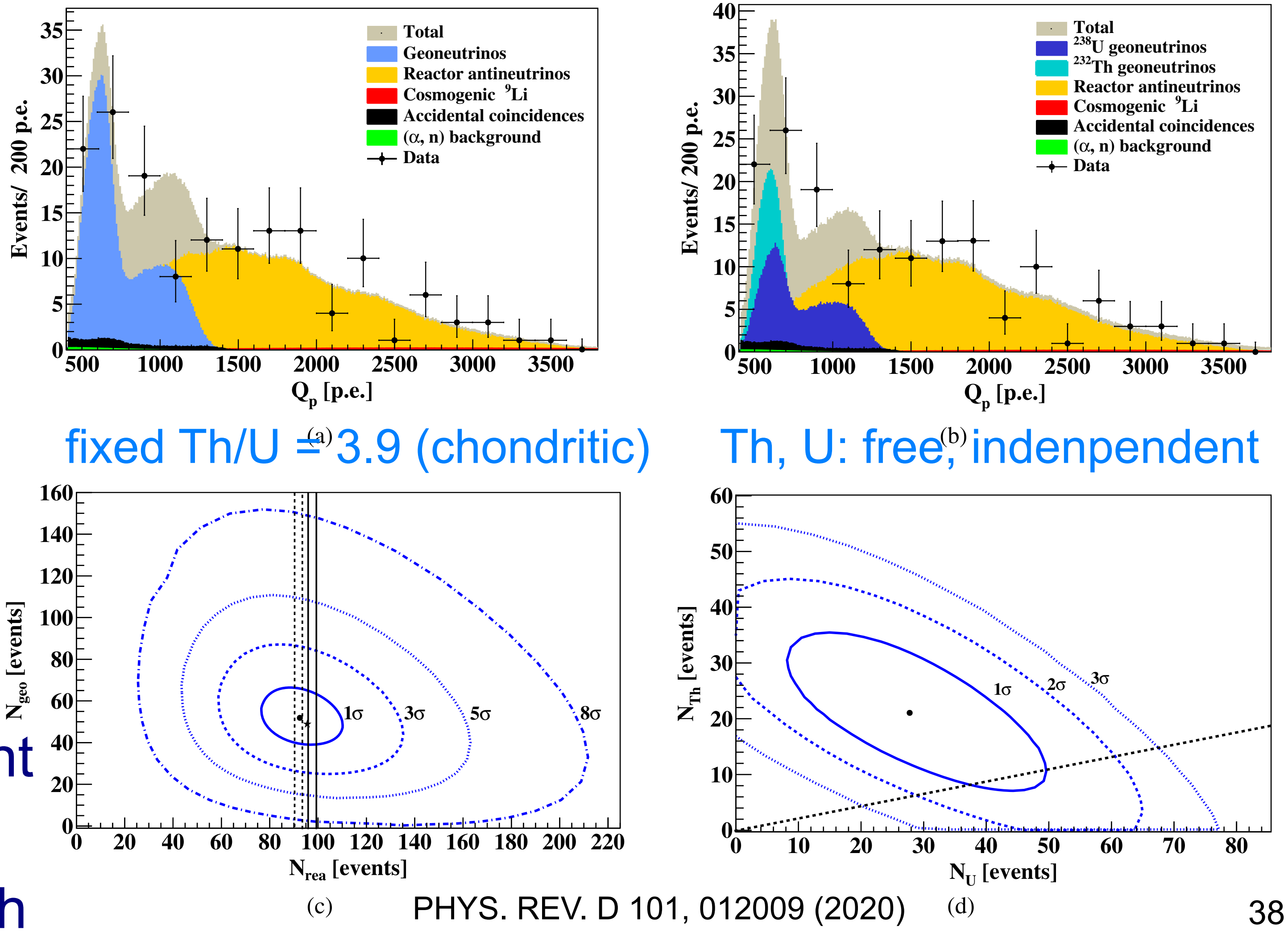

fixed Th/U = 3.9 (chondritic)

Th, U: free, indenpendent

PHYS. REV. D 101, 012009 (2020)

FIG. 48. Results of the analysis of 154 golden IBD candidates. (a) Spectral fit of the data (black points with Poissonian errors) assuming the chondritic Th/U ratio. The total fit function containing all signal and background components is shown in brownish-grey. Geoneutrinos (blue) and reactor antineutrinos (yellow) were kept as free fit parameters. Other nonantineutrino backgrounds were constrained in the fit. (b) Similar fit as in (a) but with ^{238}U (dark blue) and ^{232}Th (cyan) contributions as free and independent fit components. (c) The best fit point (black dot) and the contours for the 2D coverage of 68, 99.7, $(100–5.7 \times 10^{-5})$%, and $(100–1.2 \times 10^{-13})$%, (corresponding to 1, 3, 5, and 8σ, respectively), for N_{geo} versus N_{rea} assuming Th/U chondritic ratio. The vertical lines mark the 1σ bands of the expected reactor antineutrino signal (solid—without "5 MeV excess," dashed—with "5 MeV excess"). For comparison, the star shows the best fit performed assuming the ^{238}U and ^{232}Th contributions as free and independent fit components. (d) The best fit (black dot) and the 68, 95.5, and 99.7% coverage contours (corresponding to 1σ, 2σ, and 3σ contours) N_{Th} versus N_U. The dashed line represents the chondritic Th/U ratio.

BSE models are tested

- Various BSE (Bulk Silicate Earth) models are tested
- Borexino data (black line and grey band) shows relatively high geoneutrino signal

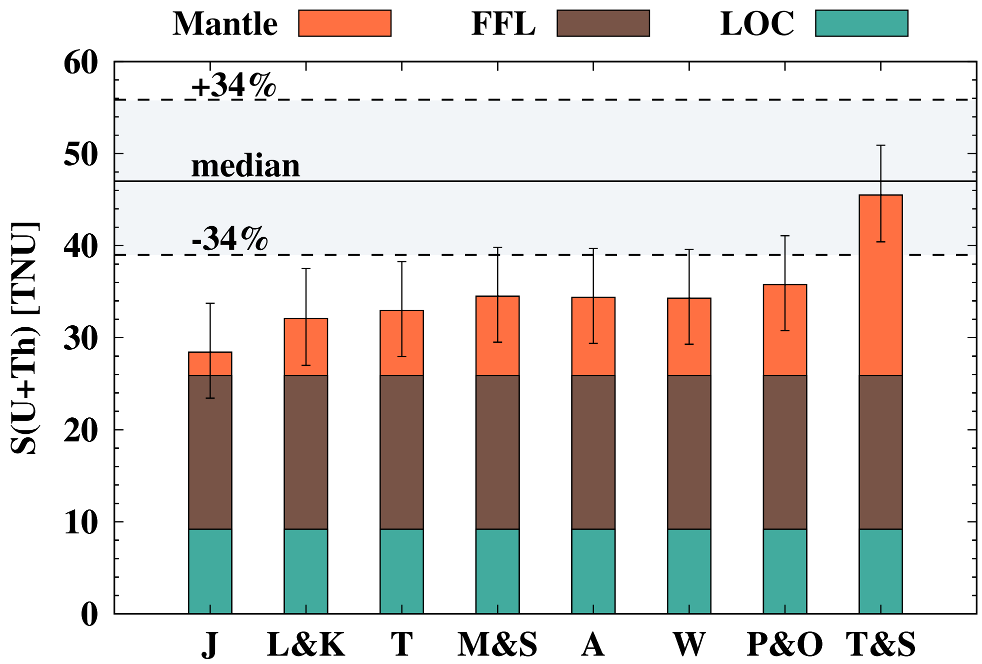

FIG. 50. Comparison of the expected geoneutrino signal $S_{geo}(U + Th)$ at LNGS (calculated according to different BSE models, see Sec. V B) with the Borexino measurement. For each model, the LOC and FFL contributions are the same (Table VI), while the mantle signal is obtained considering an *intermediate scenario* [Fig. 16(b)]. The error bars represent the 1σ uncertainties of the total signal $S(U + Th)$. The horizontal solid back line represents the geoneutrino signal S_{geo}^{med}, while the grey band the I_{Sgeo}^{68full} interval as measured by Borexino.

PHYS. REV. D 101, 012009 (2020)

Results released so far

- Results released so far are all consistent and uncertainty has been improved greatly

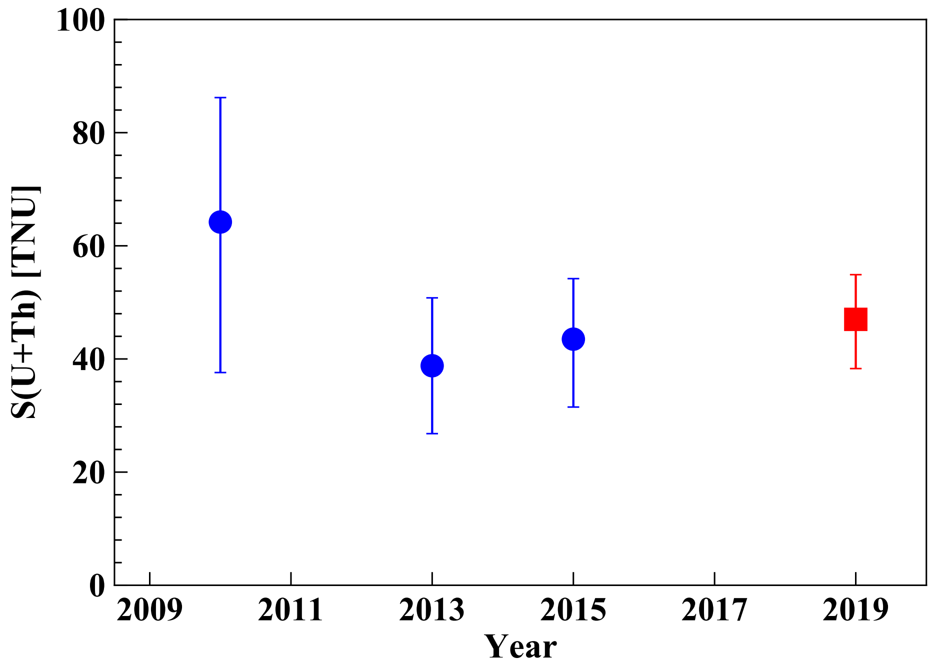

FIG. 51. Comparison of the geoneutrino signal $S_{geo}(U + Th)$ at LNGS as measured by Borexino. Blue circles indicate the results from 2010 [16], 2013 [17], and 2015 [18], while the red square demonstrates the current analysis.

PHYS. REV. D 101, 012009 (2020)

Mantle contribution significant

- Mantle contribution is clearly significant, with careful estimation of crust contribution
- In the lower panel, “0” (no mantle contribution hypothesis) is outside of the 99.7 % confidence interval.

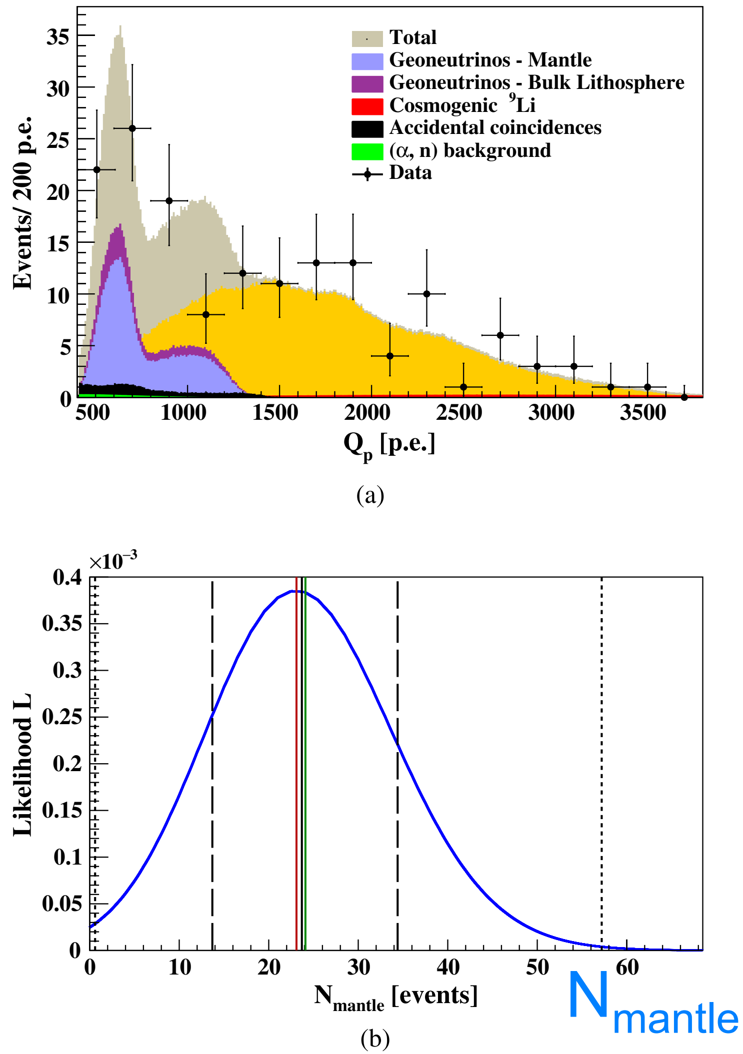

FIG. 52. (a) Spectral fit to extract the mantle signal after constraining the contribution of the bulk lithosphere. The grey shaded area shows the summed PDFs of all the signal and background components. (b) The likelihood profile for N_{mantle}, the number of mantle geoneutrino events. The vertical solid red line indicates the best fit, while the vertical solid black and green lines indicate the median and mean values of the distributions, respectively. The vertical dashed/dotted lines represent the 68%/99.7% confidence intervals of the distribution.

PHYS. REV. D 101, 012009 (2020)

Researches
by theorists and geologists

Combined analyses

- Combined analyses using both KamLAND and Borexino data are performed involving theorists and geologists.
- In an example shown here, various cases of constraints (e.g. Th/U ratio) are tested, and stability of conclusions and consistency between two data are carefully examined.

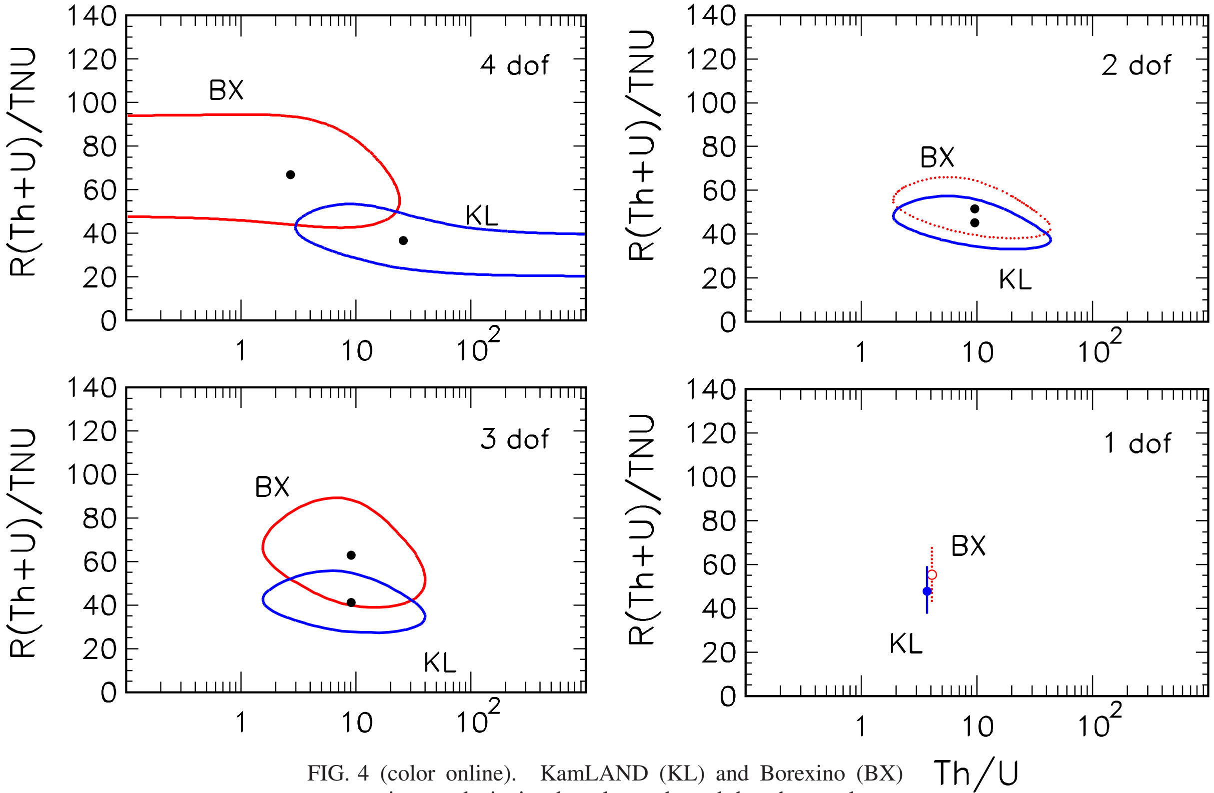

FIG. 4 (color online). KamLAND (KL) and Borexino (BX) geoneutrino analysis in the plane charted by the total rate $R(\mathrm{Th} + \mathrm{U})$ and by the mass abundance ratio Th/U. The curves represent 1σ contours ($\Delta\chi^2 = 1$) around the best-fit points (thick dots). From top to bottom, the degrees of freedom decrease from $N_D = 4$ to $N_D = 1$, as reported in Table I.

PHYSICAL REVIEW D 82, 093006 (2010)

TABLE I. Summary of adopted degrees of freedom and constraints.

N_D	Constraints	$R(\mathrm{Th+U})_{\mathrm{KL}}$	$(\mathrm{Th/U})_{\mathrm{KL}}$	$R(\mathrm{Th+U})_{\mathrm{BX}}$	$(\mathrm{Th/U})_{\mathrm{BX}}$
4	none	free	free	free	free
3	$(\mathrm{Th/U})_{\mathrm{BX}} = (\mathrm{Th/U})_{\mathrm{KL}}$	free	free	free	—
2	$(\mathrm{Th/U})_{\mathrm{BX}} = (\mathrm{Th/U})_{\mathrm{KL}}$ and $R_{\mathrm{BX}} = 1.15R_{\mathrm{KL}}$	free	free	—	—
1	$(\mathrm{Th/U})_{\mathrm{BX}} = (\mathrm{Th/U})_{\mathrm{KL}} = 3.9$ and $R_{\mathrm{BX}} = 1.15R_{\mathrm{KL}}$	free	—	—	—

Near future experiments

SNO+

- Liquid scintillator detector in Canada. Successor of SNO who measured all-flavor solar neutrino for the first time
- Construction completed. We have to stay tuned.

The SNO+ detector filled with LAB. Credit: SNO+ Collaboration
https://www.snolab.ca/news/sno-completes-lab-fill/

JUNO

- Multipurpose neutrino detector in China. (especially reactor neutrino oscillation, to further improve Daya Bay achievements)
- Largest liquid scintillator detector (20 kton) when completed
- Construction started. We look forward to their works

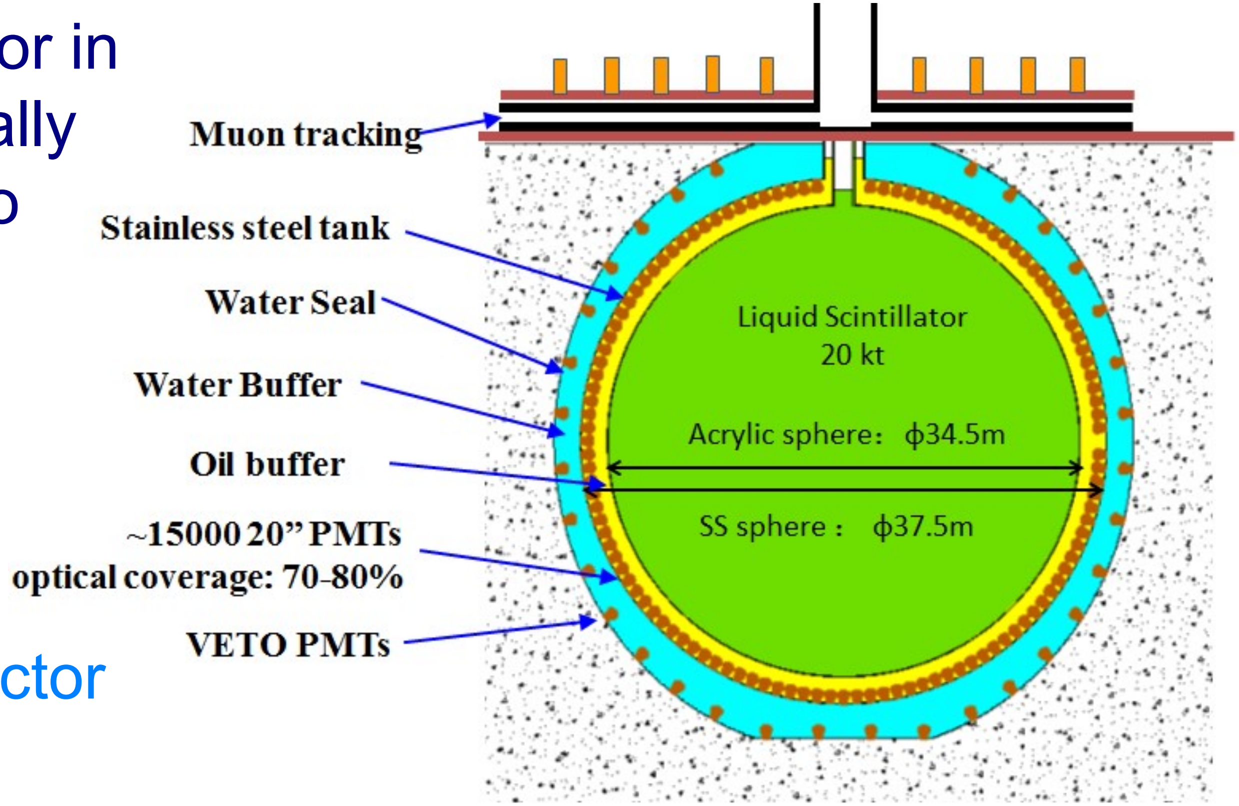

http://juno.ihep.cas.cn/

Jinping

- Plan of multipurpose neutrino detector in China
- Largest overburden (2400 m)
- To measure geoneutrinos from Himalaya (largest continental crust)

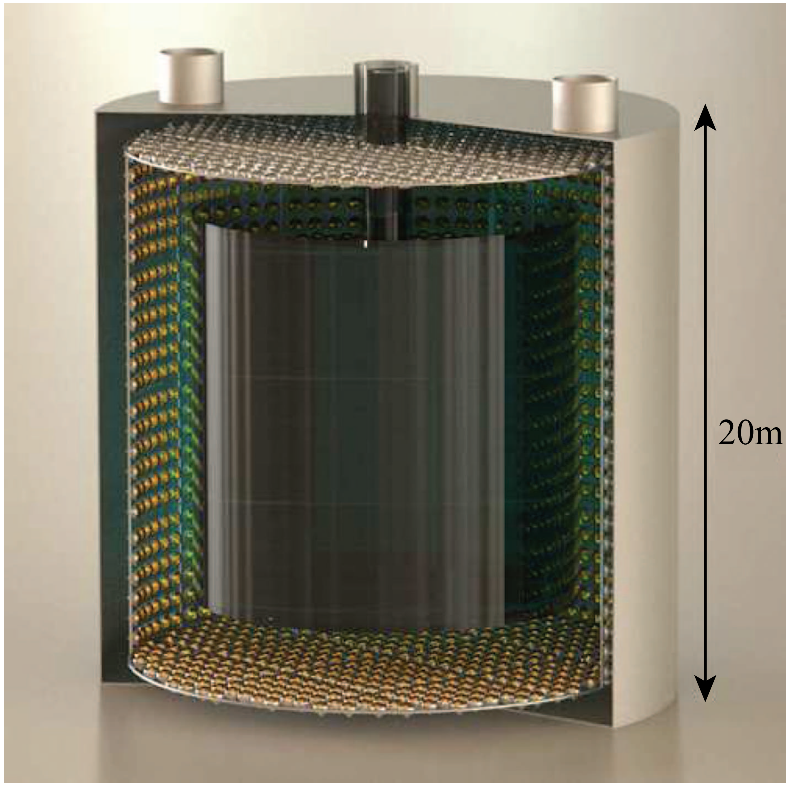

Fig. 3. (color online) The conceptual design for a cylindrical neutrino detector at Jinping. Two detectors are needed to reach the desired mass requirement.

Chinese Physics C Vol. 41, No. 2 (2017) 023002

http://jinping.hep.tsinghua.edu.cn/

Summary

- Geoneutrino measurements by KamLAND and Borexino demonstrated it is a probe to see Earth’s interior together with seismic wave

- New experiments are coming soon. We are looking forward to them